JOHN W. HUTCHINSON

a course on

NONLINEAR

FRACTURE

MECHANICS

DEPARTMENT
OF
SOLID MECHANICS

THE TECHNICAL UNIVERSITY OF DENMARK

PREFACE

A COURSE ON NONLINEAR FRACTURE MECHANICS

The notes contained within were prepared in conjunction with a
set of lectures delivered during the fall of 1978 at The Solid
Mechanics Department of the Technical University of Denmark
under the auspices of the Danish Center for Applied Mathematics
and Mechanics. Starting more or less from scratch in the sub-
ject, but assuming at least a limited knowledge of plasticity,
I have tried to bring the reader right up to some of the topics
of current interest, from both engineering and research points
of view. The section headings are listed on the next page.

John W. Hutchinson
January 5, 1979

SECTION HEADINGS

LINEAR ELASTIC FRACTURE MECHANICS

1. SOLUTIONS TO LINEAR ELASTIC CRACK PROBLEMS

References: P. Paris and G. Sih, ASTM STP 381, 1965

H. Tada, P. Paris and G. Irwin, The Stress Analysis
of Cracks Handbook, 1973.

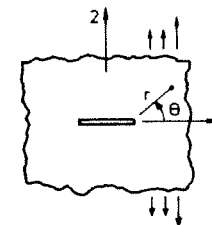H. Liebowitz (editor), Fracture, Academic Press
(7 vols.), 1971.

Isotropic, homogeneous elastic materials are assumed with E
as Young's modulus, ν as Poisson's ratio. Let $\kappa = 3 - 4\nu$ in
plane strain and $\kappa = (3 - \nu)/(1 + \nu)$ in plane stress. The
shear modulus is $G = E/[2(1 + \nu)]$.

Common to all solutions of plane problems is the
dominant singularity at the crack tip.

(i) Symmetric fields with respect to crack tip in plane
stress or plane strain (Mode I)

$$\sigma_{\alpha\beta} = \frac{K_I}{\sqrt{2\pi r}} \, \tilde{\sigma}^I_{\alpha\beta}(\theta) \tag{1.1}$$

$$u_\alpha = u^o_\alpha + \frac{K_I}{2G}\sqrt{\frac{r}{2\pi}} \, \tilde{u}^I_\alpha(\theta,\kappa) \tag{1.2}$$

where $\tilde{\sigma}^I_{22}(\theta = 0) \equiv 1$. The $\tilde{\sigma}_{\alpha\beta}(\theta)$ and $\tilde{u}(\theta)$ are given in
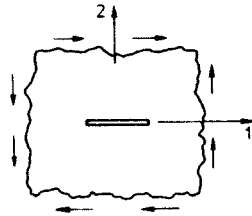almost all texts on fracture. Note that ahead of the crack

$$\sigma_{22} = K_I/\sqrt{2\pi r} \tag{1.3}$$

K_I is called the <u>stress intensity factor</u> (in Mode I).
$\sigma_{33} = 0$ in plane stress. $\sigma_{33} = \nu(\sigma_{11} + \sigma_{22})$ in plane strain.

(ii) Anti-symmetric fields with respect to crack tip in plane stress and plane strain (Mode II)

$$\sigma_{\alpha\beta} = \frac{K_{II}}{\sqrt{2\pi r}} \, \tilde{\sigma}_{\alpha\beta}^{II}(\theta) \qquad (1.4)$$

$$u_\alpha = u_\alpha^o + \frac{K_{II}}{2G} \sqrt{\frac{r}{2\pi}} \, \tilde{u}_\alpha^{II}(\theta, \kappa) \qquad (1.5)$$
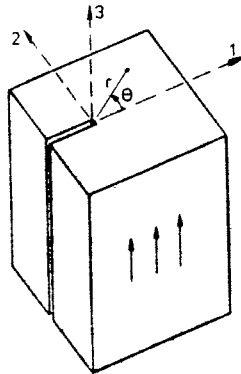

where $\tilde{\sigma}_{12}^{II}(\theta = 0) \equiv 1$ $(\sigma_{11} = \sigma_{22} = 0 , \; \theta = 0)$.

(iii) Anti-plane shear (Mode III)

$$\sigma_{3\alpha} = \frac{K_{III}}{\sqrt{2\pi r}} \, \tilde{\tau}_\alpha(\theta) \qquad (1.6)$$

$$u_3 = 2 \frac{K_{III}}{G} \sqrt{\frac{r}{2\pi}} \sin(\theta/2) \qquad (1.7)$$

where $\tilde{\tau}_1 = -\sin(\theta/2)$ and $\tilde{\tau}_2 = \cos(\theta/2)$.

In general, in any plane problem the crack tip singularity fields are a linear superposition of Mode I and Mode II. For a 3 dimensional problem, the singular stress fields, at any point along the crack edge, will be a linear superposition of Modes I and II (plane strain) and Mode III.

A large catalogue of stress intensity factors is now available. Most basic (and some not so basic) elastic crack problems seem to have been solved, either analytically or numerically. Perhaps the most complete source is the <u>Stress Analysis of Cracks Handbook</u>. Some examples are listed below.

Finite crack in infinite plane in tension

$$K_I = \sigma^\infty \sqrt{\pi a} \qquad (1.8)$$
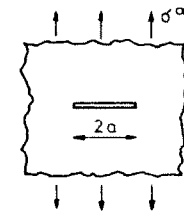
Finite crack in infinite plane in shear

$$K_I = \tau^\infty \sqrt{\pi a} \qquad (1.9)$$

Finite crack in infinite body and edge crack in half space in Mode III

$$K_{III} = \tau^\infty \sqrt{\pi a} \qquad (1.10)$$
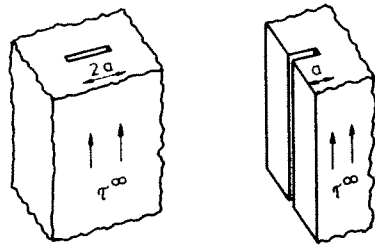
Edge crack in half plane in tension

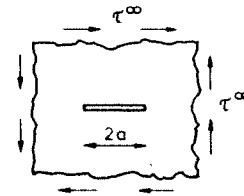$$K_I = 1.122 \, \sigma^\infty \sqrt{\pi a} \qquad (1.11)$$
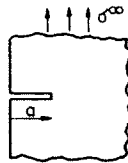
Line of cracks in tension (also Mode III)

$$K_I = \sigma^\infty \sqrt{\pi a} \left[\frac{2b}{\pi a} \tan \left(\frac{\pi a}{2b} \right) \right]^{\frac{1}{2}} \qquad (1.12)$$
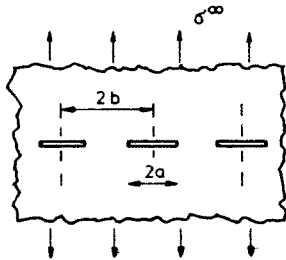
Cracks in finite width strips in Mode III

$$K_{III} = \tau^\infty \sqrt{\pi a} \left[\frac{2b}{\pi a} \tan \left(\frac{\pi a}{2b} \right) \right]^{\frac{1}{2}} \qquad (1.13)$$
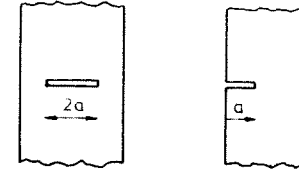
Standard ASTM compact tension specimen

P = load/unit thickness

(h = .6b , h_1 = .275b , D = .25b , c = .25b , thickness = b/2)

$$K_I = (P/b) \sqrt{a} \; F_1 (a/b) \qquad (1.14)$$
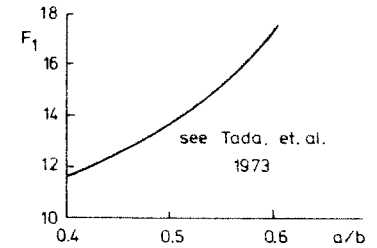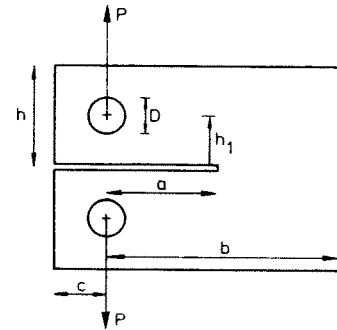
Edge crack in strip in bending
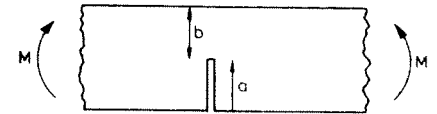
M = moment/thickness

$$K_I = Mb^{-3/2} f(a/b)$$

$$(1.15)$$

(a/b → 1 , f → 3.95)

(a/b → 0 , K → 1.122 $\sigma \sqrt{\pi a}$)

Penny shaped crack. Near crack edge fields are identical to Mode I plane strain

$$K_I = \frac{2}{\pi} \sigma^{\infty} \sqrt{\pi a} \qquad (1.16)$$
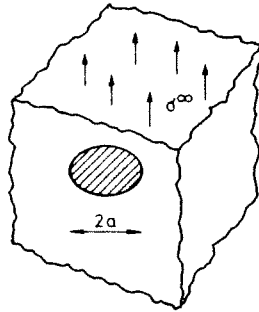
2. ENERGY RELEASE RATE, COMPLIANCE ANALYSIS, AND RELATION TO STRESS INTENSITY FACTORS

References: Tada, *et al.* 1973.

First consider <u>prescribed load</u> problems in Mode I. Let a be length of crack and P be the load per unit thickness. Let PE denote the potential energy of the system (per unit thickness) and let Δ be the load-point displacement through which P works. Denote by G the energy release rate per unit thickness, i.e.

$$G = -\left(\frac{\partial PE}{\partial a}\right)_P \qquad (2.1)$$

Now for prescribed P,

$$PE = SE - P\Delta = \tfrac{1}{2}P\Delta - P\Delta = -\tfrac{1}{2}P\Delta$$

$$G = \frac{1}{2}\frac{\partial}{\partial a}(P\Delta)\Big|_P = \frac{P}{2}\left(\frac{\partial \Delta}{\partial a}\right)_P \qquad (2.2)$$
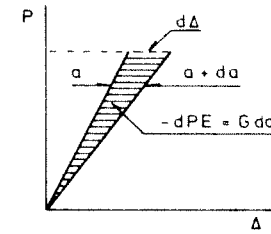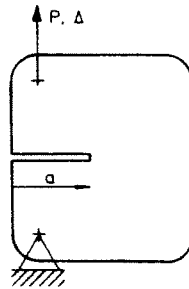
Define <u>compliance</u> C of body

$$C = \Delta/P \qquad (2.3)$$

where C depends only on geometry, E and ν.

$$\left(\frac{\partial \Delta}{\partial a}\right)_P = P\frac{dC}{da} \rightarrow G = \tfrac{1}{2}P^2\frac{dC}{da} \qquad (2.4)$$

Next consider a cracked body loaded under compliant conditions (see figure) in Mode I. Let C_M be the compliance of a spring (eg. testing machine) in series with the body. Let Δ_T be the total displacement which will be regarded as prescribed.
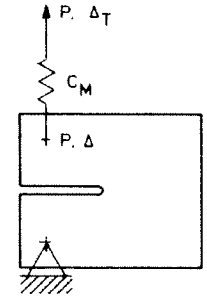
$$\Delta_T = \Delta + C_M P = \Delta + (C_M/C)\Delta \qquad (2.5)$$

Now the potential energy is

$$PE = SE + \tfrac{1}{2}C_M P^2 = \tfrac{1}{2}C^{-1}\Delta^2 + \tfrac{1}{2}C_M^{-1}(\Delta_T - \Delta)^2$$

and the energy release rate is

$$G = -\left(\frac{\partial PE}{\partial a}\right)_{\Delta_T} = -\left[C^{-1}\Delta - C_M^{-1}(\Delta_T - \Delta)\right]\left(\frac{\partial \Delta}{\partial a}\right)_{\Delta_T} + \frac{1}{2}C^{-2}\Delta^2 \frac{dC}{da}$$

<div align="right">(2.6)</div>

$$= \frac{1}{2}C^{-2}\Delta^2 \frac{dC}{da} = \frac{1}{2}P^2 \frac{dC}{da}$$

Thus the energy release rate does not depend on the nature of the loading system. Note that $C_M \to \infty$ corresponds to dead load, i.e. the previous case, and $C_M = 0$ corresponds to prescribed displacement, i.e. a rigid loading system. Eq. (2.6) is frequently used in the experimental determination of G . The compliances of two specimens, identical except for a small difference in crack length, are determined experimentally and in this way dC/da can be estimated.

The relation between G and K in Mode I is now derived. Let the body be subject to prescribed displacements (it has just been shown that G is independent of nature of loading). We will calculate the energy released during a small advance of the crack Δa . As depicted in the figure, before the crack is advanced the stress acting across the plane $y = 0$ is $\sigma_{22}(x,0)$ and for Δa small (we will later let $\Delta a \to 0$)

$$\sigma_{22}(x,0) = \frac{K(a)}{\sqrt{2\pi x}} \qquad 0 < x \le \Delta a \qquad (2.7)$$

where $K(a)$ denotes the stress intensity factor under the prescribed displacement at crack length a . The energy release during the extension, $G\Delta a$, is the negative of the work done by the traction $\sigma_{22}(x,0)$ and this is

$$G\Delta a = \frac{1}{2}\int_0^{\Delta a} \sigma_{22}(x,0)\left[V(x,0^+) - V(x,0^-)\right]dx$$

where $V(x,0^+) - V(x,0^-)$ is the separation of the crack faces in the final position when the crack is at $a + \Delta a$. From (1.2) (and any of the standard references) for Δa small

$$V(x,0^+) - V(x,0^-) = K(a + \Delta a)\frac{(1+\kappa)}{G}\sqrt{\frac{\Delta a - x}{2\pi}}$$

where $K(a + \Delta a)$ is the final value of K .
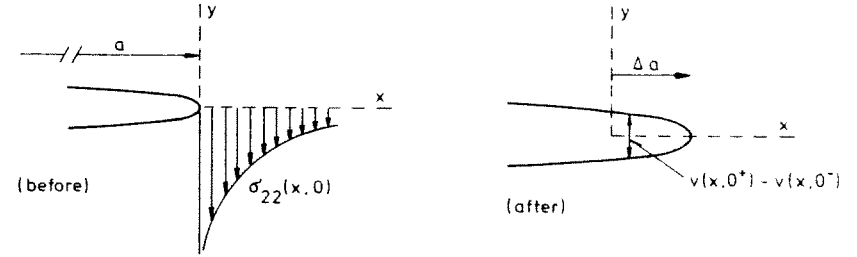
Thus,

$$G\Delta a = \frac{1+\kappa}{4\pi G}K(a)\, K(a + \Delta a)\int_0^{\Delta a}\sqrt{\frac{\Delta a - x}{x}}\,dx$$

$$= \frac{1+\kappa}{8G}K(a)\, K(a + \Delta a)\Delta a$$

and therefore $G = (1+\kappa)K^2/8G$. Using the expressions for κ one finds

$$G = \frac{1-\nu^2}{E}K^2 \qquad \text{(plane strain)} \qquad (2.8)$$

$$= \frac{K^2}{E} \qquad \text{(plane stress)} \qquad (2.9)$$

In a 3-D body with a crack edge subject to K_I , K_{II} and K_{III} , the energy release rate per unit length of crack edge is

$$G = \frac{1-\nu^2}{E}(K_I^2 + K_{II}^2) + \frac{1}{2G}K_{III}^2 \qquad (2.10)$$

3. ENERGY METHODS FOR ESTIMATING G AND K

References: Tada, *et al.* 1973.

J.R. Rice in <u>Fracture</u>, vol. 2, 1971.

As a first example consider a double cantilever beam specimen (DCB).
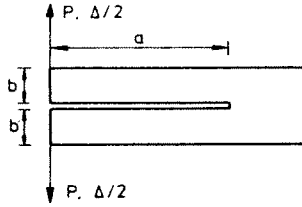
Treat each arm of the specimen as a cantilever beam of length a so that

$$\frac{\Delta}{2} = \frac{Pa^3}{3EI} = \frac{4Pa^3}{Eb^3} \rightarrow C = \frac{8a^3}{Eb^3}$$

Using (2.6) and (2.9) for plane stress gives

$$G = \frac{12P^2a^2}{Eb^3} \quad \text{and} \quad K = 2\sqrt{3}\, Pab^{-3/2} \qquad (3.1)$$

As a second example consider a semi-infinite crack in an infinite strip held in rigid grips and subject to a prescribed separation Δ .
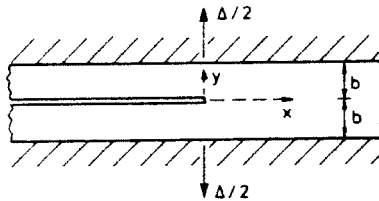
The strip is clamped in the unloaded state so that $\varepsilon_{xx} = 0$ as $|x| \rightarrow \infty$. Let the crack extend by an amount da . The stress and strain fields are unchanged if one shifts the origin in the positive x-direction by an amount da . Denote the strain energy density for $x \rightarrow +\infty$ by $(SED)^\infty$ and note that the strain energy density vanishes for $x \rightarrow -\infty$. The strain energy per unit thickness released is $(SED)^\infty 2b\, da$. Thus, since $dPE = dSE$,

$$G = 2b(SED)^\infty \qquad (3.2)$$

For example for plane stress as $x \rightarrow \infty$,

$$\varepsilon_{xx} = 0 \ , \ \varepsilon_{yy} = \Delta/2b \ , \ \sigma_{yy} = [E/(1 - \nu^2)]\Delta/2b \ , \ \sigma_{xx} = \nu\sigma_{yy}$$

and

$$(SED)^\infty = \frac{1}{2}(\sigma_{xx}\varepsilon_{xx} + \sigma_{yy}\varepsilon_{yy}) = \frac{1}{2}[E/(1 - \nu^2)](\Delta/2b)^2$$

From (3.2) and (2.9),

$$G = \frac{1}{4}\frac{E}{1 - \nu^2}\frac{\Delta^2}{b} \quad \text{and} \quad K = \frac{1}{2\sqrt{1 - \nu^2}}\frac{E\Delta}{\sqrt{b}} \qquad (3.3)$$

These are exact results. Note that the general expression (3.2) applies for a nonlinear elastic solid as well.

As a final example consider stress relief due to many cracks as shown in the figure. Assuming $b/a \ll 1$ and that the cracks extend together, show that for plane stress

$$G = \frac{Eb(\varepsilon_{yy}^\infty)^2}{2(1 - \nu^2)} \quad \text{and} \quad K = \frac{E\sqrt{b}\,\varepsilon_{yy}^\infty}{\sqrt{2(1 - \nu^2)}} \qquad (3.4)$$

where $\varepsilon_{yy}^\infty = \Delta/w$ is the strain far ahead of the cracks. Note that G is the energy release rate per crack tip and that it is independent of crack length.
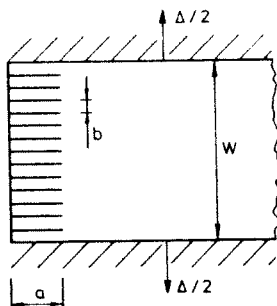
4. THE CONCEPT OF SMALL SCALE YIELDING

Linear elastic fracture mechanics is based on the concept of small scale yielding (s.s.y.). In words, s.s.y. holds when the plastic zone at the crack tip is sufficiently small (compared to the crack length and other relevant geometric length quantities) such that the elastic singularity fields of Section 1 still give a good approximation to the actual fields in an annular region surrounding the tip. This is an asymptotic condition which is increasingly violated as the load increases. The condition is depicted in Figure (4.1).
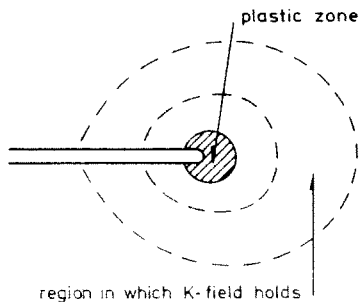
Fig. (4.1).

Under conditions of s.s.y. the stress intensity factor K (for a given mode) provides a unique measure of the intensity of the strain fields at the tip, independent of other aspects of geometry and details of loading. Considerable effort, both theoretical and experimental, has gone into the delineation of s.s.y., and this will be one side product of our later study of large scale yielding. Roughly speaking, in most instances s.s.y. appears to be a reasonable assumption as long as the applied load is below about one half of the load at which full plastic yielding occurs (i.e., the limit load for an elastic-perfectly plastic solid).

Later we will be investigating the behavior in the plastic zone under various conditions. Here we will record by way of the accompanying figure the simplest approximate shape and size of the plastic zone in s.s.y. for three Mode I conditions. In plane strain it is essential that $r_p \ll t$, where t is the thickness, and in plane stress $r_p \gg t$.
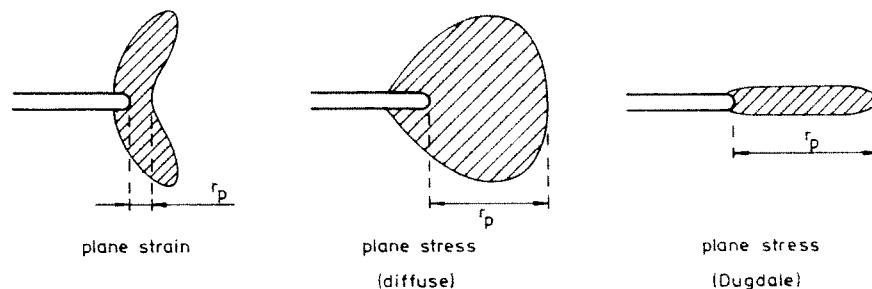
Fig. (4.2).

With σ_o denoting the tensile yield stress the results commonly used (see Tada, *et al*. pg. 1.17) are

$$r_p = (1/3\pi)(K/\sigma_o)^2 \quad \text{plane strain} \qquad (4.1)$$

$$r_p = (1/\pi)(K/\sigma_o)^2 \quad \text{plane stress (diffuse)} \qquad (4.2)$$

$$r_p = (\pi/8)(K/\sigma_o)^2 \quad \text{Dugdale model} \qquad (4.3)$$

Thus if L is the smallest relevant length (eg. crack length or uncracked ligament), s.s.y. requires $r_p \ll L$.

5. INITIATION OF CRACK GROWTH IN S.S.Y.

References: J.F. Knott, Fundamentals of Fracture Mechanics, chp. 5, Butterworths, (1973).

D. Broek, Elementary Engineering Fracture Mechanics, chp. 6, Noordhoff, (1974).

J. Carlsson, Brottmekanik, Stockholm, (1976).

Griffith's energy criterion

Consider a "perfectly brittle" material which requires a surface energy T (energy per unit area) for the creation of new surface. A necessary condition for crack propagation (in Mode I, for example) is $G \geq 2T$. Griffith proposed that fracture would occur when G attains the value $G_c = 2T$. Thus the criterion for fracture initiation (and for continued quasi-static propagation for a perfectly brittle material) can be written as

$$G = G_c \qquad (5.1)$$

where G is regarded as being applied and therefore a function of geometry and load. On the other hand, G_c is regarded as a material parameter. Using either (2.8) or (2.9) we can rewrite this as

$$K = K_c \qquad (5.2)$$

where $K_c = [EG_c/(1 - \nu^2)]^{\frac{1}{2}}$ under plane strain conditions and

$K_c = [EG_c]^{\frac{1}{2}}$ in plane stress.

Orowan and Irwin later argued that (5.1) will still apply in the presence of plastic yielding at the crack tip under s.s.y. conditions if G_c is reinterpreted as the combined energy/unit area of crack advance going into the formation of new surface area, the fracture processes and the plastic deformation. For most metals G_c interpreted this way is several orders of magnitude larger than $2T$, except under extremely brittle conditions such as at very low temperatures. As of yet it has not been possible to calculate G_c as a basic material property using data such as T , E , σ_o , initial void spacing, etc. Orowan and Irwin proposed that G_c be an experimentally determined quantity obtained using (5.1) in conjunction with the observed load at which the crack starts to grow in some test specimen.

Largely due to Irwin, the interpretation of the fracture initiation criterion shifted from the energy based condition (5.1) to one based on stress intensity (5.2). Mathematically the two approaches are entirely equivalent in s.s.y. However it is the stress intensity approach which to date has been most successfully extended to large scale yielding (nonlinear) fracture mechanics, as will later be discussed.

For the purpose of discussion suppose the compact tension specimen (1.14) is used with $a/b = 1/2$ so that $F_1 \cong 13.5$ and

$$K \cong 7.25 \, P/\sqrt{a} \qquad (5.3)$$

where P is the load/unit thickness. Assume further that the plastic zone size r_p satisfies s.s.y., i.e. $r_p \ll a$, which will be discussed further below. Next, for a given thickness t suppose the load P_c is measured associated with the onset of crack growth. Let K_c be that value of K from (5.3) at $P = P_c$. A plot of K_c as a function of t , with all tests conducted at the same temperature, is depicted in the figure (see the books by Broek, Carlsson and Knott for more details concerning experimental details, fracture surfaces, identification of initiation, etc.).
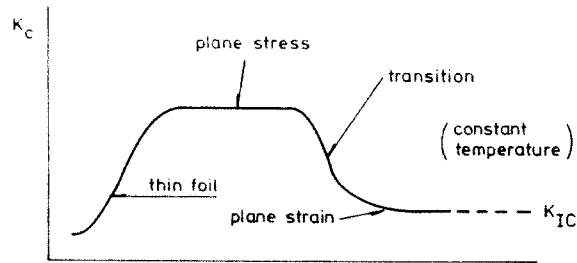
With the possible exception of some very thin foils, the lowest value of K_c at any given temperature is found for thick specimens. Then plane strain conditions prevail along most of the crack edge in the interior of the specimen. For sufficiently large thicknesses K_c is found to approach an asymptotic value which is denoted by K_{Ic} and is called the fracture toughness. The fracture toughness is a material property which characterizes the initiation of fracture at a sharp crack (sharpened by fatigue cracking at a low K-level) under Mode I, plane strain conditions. More important details of the "standard K_{Ic} test" are described in ASTM publications (ASTM Standards 31, 1969, pp. 1099-1114 and The Standard K_{Ic}-test, ASTM STP 463, 1970, pp. 249-269, and Fracture toughness testing methods, ASTM STP 381, 1965).

Recalling the size of the plastic zone r_p (4.1), plane strain conditions require $t >> r_p$. The ASTM standards for K_{Ic} testing require (validated by extensive testing)

$$t \geq 2.5 \ (K_{Ic}/\sigma_o)^2 \tag{5.4}$$

It is also required that $a >> r_p$ for s.s.y.;

$$a \geq 2.5 \ (K_{Ic}/\sigma_o)^2 \tag{5.5}$$

is usually sufficient. For example, for the compact tension specimen (5.3) the limit load for a specimen of elastic-perfectly plastic material is $P_L = \sigma_o a/6$. If the specimen is sized such that $P_C = 1/2 \, P_L$ then from (5.3) one obtains

$$a = 2.7 \ (K_C/\sigma_o)^2 \tag{5.6}$$

The fracture toughness of many metals is a strong function of temperature T. A schematic plot of K_{Ic} versus T is shown.
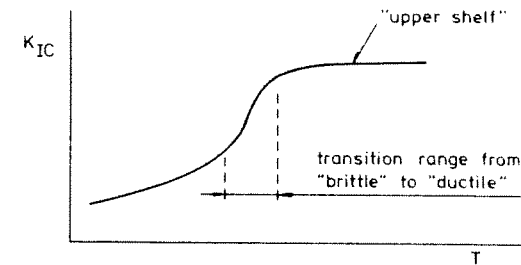
Extensive data for K_{Ic} is now available. A large compendium of fracture toughness (and fatigue) references is given by Hudson and Seward, Int. J. of Fracture 14, August 1978. A few materials are also documented in Table XIX of Formelsamling i Hållfasthetslära. Representative data for several metals is given in the table below where r_p is computed from (4.1). Also included is the crack length $L = 2a$ corresponding to fracture initiation for a finite length crack in an infinite body (1.8) where the applied stress is one half the yield stress, i.e. $\sigma^\infty = 1/2 \, \sigma_o$. That is, from (1.8)

$$L = \frac{8}{\pi} \left(\frac{K_{Ic}}{\sigma_o} \right)^2 = 24 \, r_p \tag{5.7}$$

Note that L is essentially the same as the crack length (5.5) needed to ensure a valid K_{Ic} test using the compact tension specimen.

Material	T(^{o}C)	σ_o (MN/m^2)	K_{Ic} (MN/m$^{3/2}$)	r_p (mm)	L(mm)
6061-T651 (Aℓ)	20	269	33	5	120
7075-T651 (Aℓ)	20	620	36	.35	8.4
AISI 4340	0	1500	33	.05	1.2
A 533-B	93	620	200	11	260

TABLE (5.1)

(intended for illustrative purposes only)

The combination of high toughness and low yield stress leads
to relatively large values of the plastic zone size at fracture
and also relatively long cracks necessary to lead to initia-
tion of growth at a given stress level which is some fraction
of the general yield stress. It must also be remenbered that
K_c for plane stress conditions is often much higher than K_{Ic} .

6. CRACK GROWTH AND STABILITY IN S.S.Y.

In a perfectly brittle material we expect the condition for
the initiation of crack growth and for continuation of growth
to be $K = K_c$ where K_c remains constant. This is depicted
in Figure (6.1a) where the K needed to propagate the crack
is plotted against the crack advance Δa . To a first approxi-
mation such behavior is typical of high strength, low toughness
metals under plane strain conditions. By proper selection of

Fig. 6.1a.   Fig. 6.1b.

specimen configuration it is possible to measure experimental-
ly behavior such as that in Fig. (6.1a). For example, a finite
crack in an infinite plane
loaded by concentrated loads as
shown has a stress intensity
factor which decreases with in-
creasing a when P is held
fixed:

$$K = P/\sqrt{\pi a} \qquad (6.1)$$

(Tada, *et al.*, pg. 5.4) .

Thus, $K = K_c$ implies that P must increase with crack advance according to
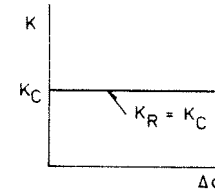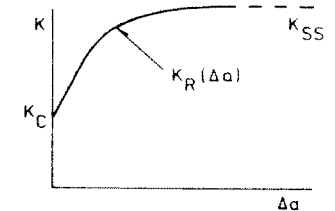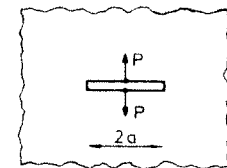
$$P = K_c\sqrt{\pi(a_0 + \Delta a)} = P_c\sqrt{1 + \Delta a/a_0} \qquad (6.2)$$

where a_0 is the initial crack length and P_c is the initiation load.

The behavior sketched in Fig. (6.1b) is more representative of intermediate and low strength metals under plane stress or plane strain conditions. It can also be seen in some of the high strength metals under plane stress conditions. Here crack advance takes place under increasing applied K. In s.s.y., assuming also that Δa is small compared to relevant geometric lengths, $K_R(\Delta a)$ is a curve which characterizes the material under a given set of conditions, eg. temperature, plane stress or plane strain, etc. It is called the <u>resistance curve</u> or <u>R-curve</u> ("The R-curve", A.S.T.M. S.T.P. - 527, 1974). (A note on notation. I will use K_c, and later J_c, to denote initiation. Some authors use K_c to denote the instability value of K. It is also commonplace to use $G = R(\Delta a)$ to describe the resistance curve. I will use $K = K_R(\Delta a)$). The value of K needed to give continued, steady-state crack propagation, K_{ss}, is often many times K_c. For low and intermediate strength steels small crack advances of, say, 1 or 2 mm can lead to values of K_R which are twice K_{Ic} under plane strain conditions, as will be discussed further later in the notes.

The condition for <u>continued crack advance</u>, given that the current crack length is $a_0 + \Delta a$, is

$$K = K_R(\Delta a) \qquad (6.3)$$

where K on the left hand side of (6.3) is regarded as the "applied" K. The condition for <u>stability of crack advance</u> is

$$\left(\frac{\partial K}{\partial a}\right)_L < \frac{d K_R}{d \Delta a} \qquad (6.4)$$

and instability becomes possible when

$$\left(\frac{\partial K}{\partial a}\right)_L = \frac{d K_R}{d \Delta a} \qquad (6.5)$$

where the partial derivatives of K with respect a are to be taken with the prescribed loading conditions held fixed. Eq. (6.4) insures that a small accidential advance of the crack under the prescribed loading conditions does not give rise to an applied K which exceeds K_R, i.e. that exceeds the resistance of the material. The transitition from stable to unstable behavior is depected in the "R-curve analysis" in the accompanying figure. There $K(L_i, a)$ denotes K as a function of a at fixed values of the loading condition L_i $(L_1 < L_2 < L_3 < L_4)$. This could be a prescribed load condition or a prescribed displacement condition. The value of K at
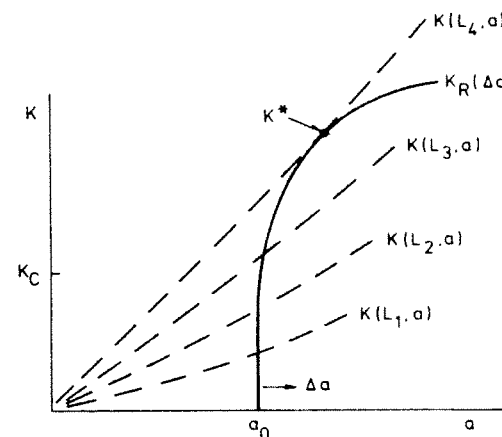
instability, K^*, depends on the loading conditions as well as the R-curve. In the figure the value of the load at instability is that associated with L_4.

Consider the specimen (or cracked component) loaded in a compliant machine shown on pg. 7. Again, let $C(a)$ denote the compliance of the specimen and let C_M denote the compliance of the loading device. The total displacement Δ_T is taken to be <u>prescribed</u> where

$$\Delta_T = \Delta + C_M P = \left(C(a) + C_M\right)P$$

Here and in section 2 the compliance $C_M = \Delta_M/P$ is also defined in terms of the force/unit specimen thickness P. If $\overline{C}_M$ is the total compliance of the loading device and t is the specimen thickness, then

$$C_M = \overline{C}_M t \qquad (6.6)$$

The stress intensity factor can aways be written as

$$K = f(a)P \qquad (6.7)$$

where $f(a)$ is assumed known and the dependence on unchanging parameters is left implicit. For analysing stability we need $(\partial K/\partial a)_{\Delta_T}$. Noting

$$dK = f dP + f'P da$$

and

$$d\Delta_T = (C + C_M)dP + C'P da = 0 ,$$

we obtain

$$\left(\frac{\partial K}{\partial a}\right)_{\Delta_T} = Pf' - \frac{PfC'}{C + C_M} \qquad (6.8)$$

Thus, while K itself and the condition for continued growth does not depend on the compliance of the loading device, stability of growth is often strongly dependent on the compliance. For <u>dead loading</u> ($C_M \to \infty$ and P is constant), (6.8) becomes

$$\left(\frac{\partial K}{\partial a}\right)_{\Delta_T} = \left(\frac{\partial K}{\partial a}\right)_P = Pf' \qquad (6.9)$$

while for <u>prescribed displacement</u> of the specimen (i.e. a rigid loading device with $C_M = 0$)

$$\left(\frac{\partial K}{\partial a}\right)_{\Delta_T} = \left(\frac{\partial K}{\partial a}\right)_\Delta = Pf' - \frac{PfC'}{C} = PC\left(\frac{f}{C}\right)' \qquad (6.10)$$

Note that, generally, $(\partial K/\partial a)_\Delta < (\partial K/\partial a)_P$, as expected, since usually $C' > 0$.

As an example, consider the D.C.B. specimen of pg. 10 where

$$C(a) = 8(a/b)^3/E \quad \text{and} \quad f(a) = 2\sqrt{3}\, ab^{-3/2}$$

Using (6.8) one finds

$$\left(\frac{\partial K}{\partial a}\right)_{\Delta_T} = 2\sqrt{3}\, Pb^{-3/2}\left[1 - \frac{3}{(1 + C_M/C)}\right] \qquad (6.11)$$

Note that the ratio C_M/C determines whether K increases or decreases with increasing a under prescribed Δ_T. The two limits, $C_M \to \infty$ and $C_M \to 0$, give, respectively,

$$(\partial K/\partial a)_P = 2\sqrt{3}\, Pb^{-3/2} = K/a \qquad (6.12a)$$

$$(\partial K/\partial a)_\Delta = -4\sqrt{3}\, Pb^{-3/2} = -2K/a \qquad (6.12b)$$

Under prescribed displacement crack growth in the D.C.B. specimen will always be stable assuming that the resistance curve does not have a negative slope. It is also assumed here that the crack advances in its plane, which is not always the case. Under dead load the crack becomes unstable, from (6.5) and (6.12a), when $K = aK'_R$ where K'_R is the local slope of the R-curve. For a brittle material such as that in Fig. (6.1b), $K'_R = 0$ and instability occurs at initiation in dead loading.

For the standard compact tension specimen it is possible to calculate $(\partial K/\partial a)_{\Delta_T}$ using numerical information from Tada, *et al.* pg. 2.20. In nondimensional form Eq. (6.8) can be written as

$$\frac{\sqrt{a}\, b}{P}\left(\frac{\partial K}{\partial a}\right)_{\Delta_T} = g_1(a/b) - (1 + C_M/C)^{-1}g_2(a/b) \qquad (6.13)$$

where a and b are defined in the figure on page 5. C is the compliance (based on a unit specimen thickness) which was approximated from Tada, *et al.* pg. 2.20 as

$$C = v_2(a/b)/\bar{E}$$

where $\bar{E} = E$ for plane stress and $\bar{E} = E/(1 - v^2)$ for plane strain. Values of g_1 and g_2 are given in the Table below, (I am indebted to Mr. H.L. Toftegaard for performing these calculations). Since $g_1 - g_2$ is negative for the range of a/b considered, a specimen of perfectly brittle material in a rigid machine $(C_M = 0)$ will not display instability. On the other hand for values of the compliance ratio greater than $(C_M/C)^*$ given in the Table, such a specimen will be unstable at initiation. With $\bar{C}_M$ as the total machine compliance and noting (6.6), one finds

$$C_M/C = \bar{E} t \bar{C}_M/v_2(a/b)$$

The larger the specimen (assuming t scales with a), for a given machine, the larger is C_M/C and therefore the more likely initiation will be unstable.

a/b	g_1	g_2	$(C_M/C)^*$
.3	6.0	16.6	1.76
.4	11.6	21.6	.86
.5	20.2	33.7	.66
.6	41.7	60.2	.44
.7	93.	132.	.41

Table (6.1).

Next consider a finite crack of length 2a in an infinite body subject to stress σ^∞ far from the crack; this is the prototype crack problem in many applications. From (1.8), $K = \sigma^\infty \sqrt{\pi a}$. When the crack is small compared to the size of the body, there is no distinction between prescribed stress or

prescribed displacement. (More precisely, for a very large body compared to the crack size, C'/C is small and the second term can be neglected in (6.8)). The relevant derivative for the instability analysis is

$$\left(\frac{\partial K}{\partial a}\right)_{\sigma^\infty} = \frac{\sigma^\infty}{2}\sqrt{\frac{\pi}{a}} = \frac{1}{2}\frac{K}{a} \tag{6.14}$$

Thus the condition for stability, once the crack has grown an amount Δa with $K = K_R$, is

$$K/2a < K'_R \tag{6.15}$$

At <u>initiation</u>, it follows from (6.15) that stability is ensured if

$$2a > K_C/(K'_R)_c \tag{6.16}$$

For many relative brittle materials (6.16) will be violated at typical crack lengths; (6.16) will be violated at all crack lengths if $(K'_R)_c = 0$. Note that the right hand side of (6.16) depends only on material properties. If $(K'_R)_c > 0$, (6.16) implies that long cracks are stable at initiation and small cracks are unstable assuming s.s.y. holds over the entire range of lengths. Of course, since $K = \sigma^\infty\sqrt{\pi a}$, a long crack starts growing at a lower applied stress than a short crack. For an R-curve such as that of Fig. (6.1b) $\ell = K_C/(K'_R)_c$ is the crack advance at which $K_R = 2K_C$, estimated using the initial slope of the R-curve. Therefore, according to (6.16), initial crack growth will be stable of the total crack length 2a is greater than the material-based length ℓ . For a brittle material ℓ will be very long but for an intermediate strength metal above the brittle-ductile temperature ℓ will usually be less than a centimeter (additional data will be given later). For such metals <u>initial</u> crack growth will therefore generally be stable at least when s.s.y. applies.

Eq. (6.8) brings out the importance of compliance on stability. We end this section by displaying a decomposition

of the compliance of a typical _finite_ body with a crack of length a , which is sometimes very useful. Let C_{nc} denote the compliance of the body without a crack, i.e. with $a = 0$. With $C(a)$ as the total compliance in the presence of the crack, define the contribution due to the crack as

$$C_{cr}(a) = C(a) - C_{nc} \qquad (6.17)$$

To illustrate the decomposition consider a beam of width b and length L subject to a moment M per unit thickness. As illustrated in the figure let θ be the load-point rotation and let θ_{nc} be the rotation with $a = 0$. Thus,

$$\theta_{nc} = ML/\bar{E}I \quad \text{and} \quad C_{nc} = L/\bar{E}I \qquad (6.18)$$
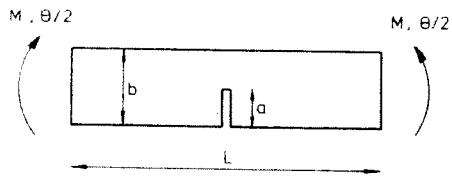
where $I = b^3/12$, $\bar{E} = E$ in plane stress and $\bar{E} = E/(1 - \nu^2)$ in plane strain. For L/b greater than about 2 or 3 $C_{cr}(a)$ in (6.17) is essentially independent of L . That is, for $L \gg b$,

$$C_{cr} = \frac{\theta_{cr}}{M} = \frac{1}{\bar{E}b^2} \, f(a/b) \qquad (6.19)$$

The function $f(a/b)$ involves the solution to the crack problem and is given in Tada, _et al._ pg. 2.14. For a _deeply-cracked specimen_ with $c \equiv b - a \ll b$ the result for C_{cr} is

$$C_{cr} = 16/(\bar{E}c^2) \qquad (6.20)$$

depending only on the uncracked ligament c . Thus we can use (6.17), together with (6.18) and (6.19), to obtain the total compliance of a specimen of any length, as long as L is not less than, say, $3b$. Tabulated results for C_{cr} for various geometries are given in Tada, _et al._

7. OTHER APPLICATIONS OF LINEAR ELASTIC FRACTURE MECHANICS

The stress intensity factor from linear elastic crack problems is used in correlating data on fatigue crack growth, creep crack growth and corrosion cracking. It is essential that s.s.y. holds in some appropriate form which guarantees that the K-fields of the elastic solution still give a good approximation to the actual fields in some region surrounding the crack tip. We will give a very brief discussion of fatigue crack growth as an illustration, leaving a more detailed treatment of this topic to a later chapter of the notes.

Consider Mode I, plane strain crack growth in s.s.y. where the crack tip experiences a stress intensity history of cyclic loading with K in the range $0 \leq K \leq \Delta K$ as depicted in the figure. If the rate of crack growth per cycle, da/dN , is measured over a range of ΔK from just below K_{Ic} to a small fraction of K_{Ic} , data such as that shown in the figure is obtained. The measurements are all made at the same temperature and it is understood that da/dN represents the rate after the growth has reached steady state. (Data of this kind is available for many metals over a range of temperatures – see, for example, the compendium of Hudson and Seward, cf. pg. 17 of notes. For a recent paper on the subject see for example R. Ritchie, J. Eng. Mat. Tech. (ASME) 1977, $\underline{99}$, 194). At values of ΔK approaching K_{Ic} the growth rate is high. At sufficiently low values of ΔK , usually less than about $K_{Ic}/10$, the growth rate in some materials is observed to be exceeding low and a threshold level ΔK_0 can be identified. In a middle range between ΔK_0 and K_{Ic} the data often can be fit by a relation of the form (Paris's Law)

$$da/dN = C(\Delta K)^m \qquad (7.1)$$

where m is typically between 2 and 4 .

The argument for the relevance of the stress intensity factor K in <u>correlating</u> fatigue growth data in s.s.y. is similar to that made in the case of monotonic loading. Given plane strain, Mode I, for example, the history of deformation at the crack tip depends on the external geometry and the loading history only through the history of K . Since the plastic zone size r_p is proportional to $(K/\sigma_0)^2$, the small scale yielding assumption is usually met without difficulty at low growth rates where ΔK is well below K_{Ic} .

The stress intensity factor is also used to correlate growth-rates under nonsteady loading cycles. The effects of overloads and nonzero minimum K in the cycle have been extensive studied and will be discussed later. In applications of fracture mechanics it is commonplace to use fatigue growth rate data to predict the length of crack as a function of load cycles. This information is used in conjunction with the fracture conditions under static (monotonic) loading, using larger static load levels for example, to estimate the lifetime of a component with some assumed initial crack size. Alternatively, inspection methods are used to determine cracks over a certain minimum size and the combined fracture mechanics approach is used to estimate the remaining lifetime of the cracked component.
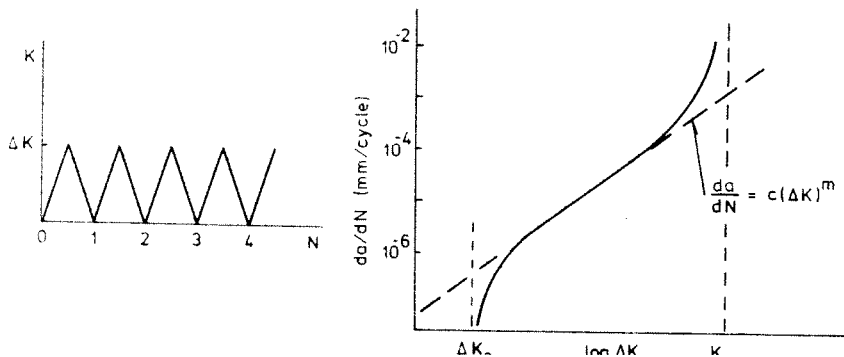
NONLINEAR FRACTURE MECHANICS

This section deals with plasticity aspects of fracture mechanics for the case of monotonic loads. The s.s.y. restriction places rather severe limitations on the applicability of linear fracture mechanics, effectively excluding its applicability to low and intermediate strength metals. Ways for extending the validity of linear elastic fracture mechanics were sought very early in the development of the subject, particularly in the analysis of plane stress crack growth where the intensity levels are higher, with associated larger plastic zone sizes, than in plane strain. In large scale yielding (l.s.y.) it is no longer possible to use solutions to linear elastic crack problems; elastic-plastic solutions must be used in their place. In the following sections of the notes several aspects of nonlinear fracture mechanics are developed. Crack tip fields in the plastic zone are determined under small and large scale yielding. The J-integral is introduced and used to extend fracture mechanics into the large scale yielding range. Limitations of the approach are discussed. Stable crack growth is shown to be a consequence of crack tip plasticity. Conditions under which it is possible to use a J-resistance curve to analyse the stability of limited amounts of crack growth will be discussed. The current status of nonlinear fracture mechanics will be reviewed.

8. THE J-INTEGRAL

References: J.R. Rice in <u>Fracture</u> Vol. 2, 1971.

B. Budiansky and J. Rice, J. Appl. Mech., 1973, pg. 201.

The J-integral found by Rice plays an important role in non-linear fracture mechanics. It is introduced in this section. We consider homogeneous bodies characterized by a deformation theory of plasticity (i.e., a small strain, nonlinear elastic

solid) with a strain energy density function $W(\varepsilon_{ij})$ such that

$$\sigma_{ij} = \partial W/\partial \varepsilon_{ij} \qquad (8.1)$$

Consider the cracked body in Fig. (8.1) in series with a nonlinear elastic spring where the load quantity P (per unit thickness of specimen) in the spring is given by

$$P = U'(\Delta_M) \quad , \quad (\ )' \equiv d(\ )/d\Delta_M \qquad (8.2)$$

where Δ_M is the elongation quantity of the spring through which P works and U is the strain energy in the spring per unit specimen thickness. Let the total displacement

$$\Delta_T = \Delta + \Delta_M \qquad (8.3)$$

be prescribed. The nonlinear elastic system of Fig. (8.1) has the potential energy

$$PE = SE(\Delta , a) + U(\Delta_M) \qquad (8.4)$$

where SE is the strain energy per unit thickness in the body given in terms of the generalized load and displacement by

$$SE(\Delta , a) = \int_0^\Delta P(\tilde{\Delta} , a)\,d\tilde{\Delta} \qquad (8.5)$$

For crack advance in the plane of the crack (i.e. in the x_1-direction) define J as the energy release rate per unit thickness according to

$$J = - \left(\frac{\partial PE}{\partial a}\right)_{\Delta_T} \qquad (8.6)$$

From (8.4), (8.2) and (8.5),
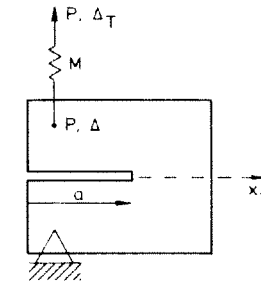
Fig. (8.1).

$$dPE = \left(\frac{\partial SE}{\partial a}\right)_\Delta da + \left(\frac{\partial SE}{\partial \Delta}\right)_a d\Delta + U'd\Delta_M$$

$$= \left(\frac{\partial SE}{\partial a}\right)_\Delta da + P(d\Delta + d\Delta_M) = \left(\frac{\partial SE}{\partial a}\right)_\Delta da$$

where the last equality holds for $d\Delta_T = 0$. Thus, from (8.6) and using (8.5),

$$J = - \left(\frac{\partial SE}{\partial a}\right)_\Delta = - \int_0^\Delta \frac{\partial P}{\partial a}(\tilde{\Delta} , a)\,d\tilde{\Delta} \qquad (8.7)$$

It is important to note that J is independent of the characteristics of the spring M and therefore it follows that (8.7) holds in the limiting cases of dead load and prescribed Δ . For a linear elastic body with $C \equiv \Delta/P$ one can readily verify that J reduces to G given by (2.6).

An alternative expression to (8.7) can be obtained by directly considering the body under dead load P . Now regard Δ as a function of P and a and integrate (8.5) by parts to get

$$SE(P , a) = P\Delta - \int_0^P \Delta(\tilde{P} , a)\,d\tilde{P}$$

Since now $PE = SE - P\Delta$,

$$PE = - \int_0^P \Delta(\tilde{P} , a)\,d\tilde{P} \qquad (8.8)$$

and

$$J = -\left(\frac{\partial PE}{\partial a}\right)_P = \int_0^P \frac{\partial \Delta}{\partial a}(\tilde{P}, a)\, d\tilde{P} \qquad (8.9)$$

Graphical interpretations of J in (8.7) and (8.9) are given in the two figures below.
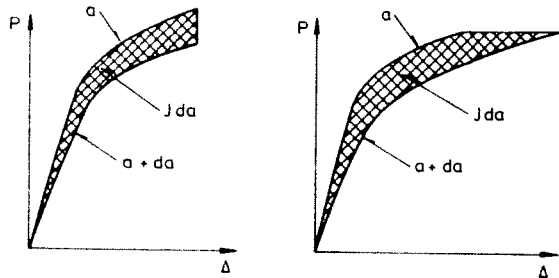
The above expressions for J are in terms of overall load-displacement quantities. We now obtain the J-integral expression involving details of the stresses and displacement gradients in the cracked body. (The derivation given below is similar to that of Budiansky and Rice, 1973. See Eshelby (Solid State Physics, Vol. III, eds. Seitz and Turnbull, Academic Press, 1956) for a different derivation within the context of finite strain, nonlinear elasticity).

First we show the important path-independence of a certain line integral. We consider plane strain, plane stress or anti-plane shear with stress and strain related by (8.1). Let σ_{ij}, ε_{ij} and u_i be any solution to the field equations involving no singularities within or on Γ. Define the line integral around Γ by
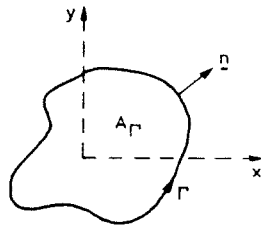
$$I_\Gamma = \int_\Gamma (Wn_x - \sigma_{ij}n_j u_{i,x})\, ds \qquad (8.10)$$

where $\underset{\sim}{n}$ is the unit outward normal to Γ. Using the divergence theorem, equilibrium and (8.1), one finds

$$\int_\Gamma Wn_x\, ds = \int_{A_\Gamma} W_{,x}\, dA = \int_{A_\Gamma} \sigma_{ij}\varepsilon_{ij,x}\, dA$$

$$= \int_{A_\Gamma} (\sigma_{ij}u_{i,x})_{,j}\, dA = \int_\Gamma \sigma_{ij}n_j u_{i,x}\, ds \qquad (8.11)$$

Thus $I_\Gamma = 0$ where A_Γ is any simply connected region containing no singularities.
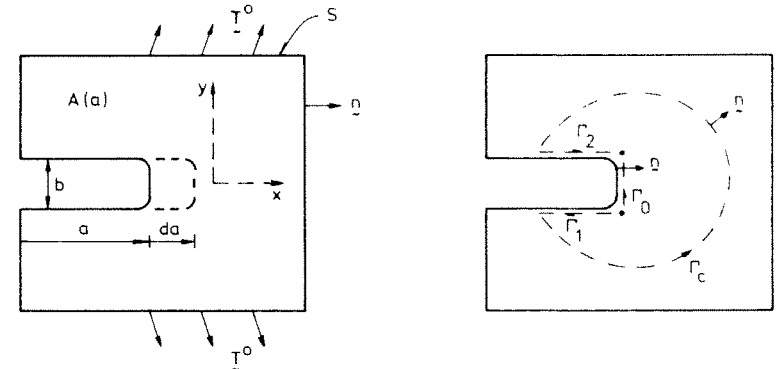
Next consider solutions to the problem shown in the figure where the region $A(a)$ is a function of a due to translation in the x-direction of the blunt-ended notch shown. The notch is traction free, while $\underset{\sim}{T}^o$ is prescribed on S_T and $\underset{\sim}{u}^o$ is prescribed on S_u. The potential energy of the system at a given a is

$$PE(a) = \int_{A(a)} W(\underset{\sim}{\varepsilon})\, dA - \int_{S_T} T_i^o u_i\, ds$$

where $\underset{\sim}{u}(\underset{\sim}{x}, a)$ and $\underset{\sim}{\varepsilon}(\underset{\sim}{x}, a)$ are the equilibrium displacement

and strain fields. Under the prescribed conditions L , with $(\dot{\ }) = (\partial(\ )/\partial a)_L$,

$$\dot{PE} = - \int_{\Gamma_0} W n_x ds + \int_A \dot{W} dA - \int_{S_T} T_i^0 \dot{u}_i ds$$

But from manipulations similar to those in (8.11),

$$\int_A \dot{W} dA = \int_A (\partial W/\partial \epsilon_{ij}) \dot{\epsilon}_{ij} dA = \int_S \sigma_{ij} n_j \dot{u}_i dS = \int_{S_T} T_i^0 \dot{u}_i dS$$

(This can also be noted immediately from the principle of virtual work). Thus,

$$\dot{PE} = - \int_{\Gamma_0} W n_x ds = - \int_{\Gamma_0} (W n_x - \sigma_{ij} n_j u_{i,x}) ds \qquad (8.12)$$

where the second part of the last integrand vanishes on Γ_0 $(\sigma_{ij} n_j = 0)$. Now use the line integral (8.10) where $\Gamma = \Gamma_1 + \Gamma_2 + \Gamma_c - \Gamma_0$, noting that the integrand of (8.10) vanishes identically along Γ_1 and Γ_2 . Thus, since $I_\Gamma = 0$,

$$\dot{PE} = - \int_{\Gamma_c} (W n_x - \sigma_{ij} n_j u_{i,x}) ds \qquad (8.13)$$

Thus the "energy release rate" for the family of blunt-ended notches is given by the line integral about <u>any</u> contour Γ_c which circles the notch as shown in the figure. We now argue (heuristically) that, by choosing a contour Γ_c remote from the end of the notch and by going to the limit of a crack $(b \rightarrow 0)$, the result (8.13) gives the desired energy release rate for the crack, i.e.

$$J = \int_{\Gamma_c} (W n_x - \sigma_{ij} n_j u_{i,x}) ds \qquad (8.14)$$
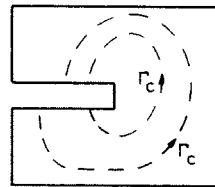
While this expression has been derived for a given set of pre-scribed loading conditions, we have previously shown that the same expression must hold for loads applied under compliant conditions.

In s.s.y. the contour Γ_c can be chosen to fall within the annular region in which the K-fields hold (see Fig. (4.1)). Then the integrand in (8.13) can be evaluated in terms of (1.1) and (1.2) of the K-fields. A direct calculation of this kind verifies (2.8) and (2.9), i.e. in Mode I

$$J = G = K^2/\bar{E} \qquad (8.15)$$

9. THE DUGDALE - BARENBLATT MODEL

References: D.S. Dugdale, J. Mech. Phys. Solids <u>8</u>, 1960, pg. 100.
G.I. Barenblatt, Adv. in Appl. Mech. <u>7</u>, 1962.
J.R. Rice in <u>Fracture</u>, Section IV, C, 1968.

Dugdale observed that the plastic zone ahead of a crack tip in a thin sheet of mild steel involved primarily cross-slip on planes at 45^0 to the plane of the sheet as indicated in Fig. (9.1).
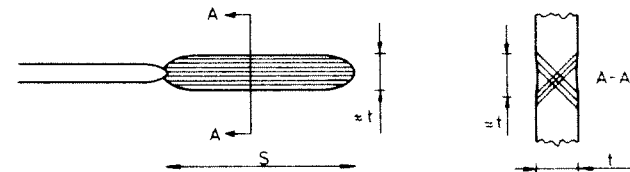
Fig. (9.1).

Assuming the length of the plastic zone s is long compared to the thickness of the sheet t , the plastic zone can be visualized as a narrow strip of height in the plane of the sheet which is approximately t . Regard the material as being elastic-perfectly plastic and take the stress σ_{yy} in the strip (i.e. along the x-axis in the yielded strip) to be the

in-plane, plane strain tensile yield stress σ_0 . As shown in Fig. (9.2) the problem is modelled by a elastic plane stress problem where the length of the plastic zone s is not yet determined. The crack is of length $2a$; the sheet is infinite;

Fig. (9.2).

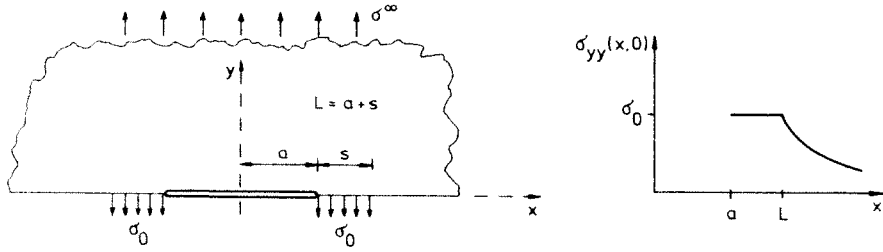and the applied stress far from the crack is $\sigma_{yy} = \sigma^\infty$. Only the upper half of the sheet is shown in Fig. (9.2). The boundary conditions along $y = 0$ are : $\sigma_{xy} = 0$ all x , $\sigma_{yy} = 0$ for $|x| < a$, $\sigma_{yy} = \sigma_0$ for $a < |x| < L$, and $v = 0$ for $|x| \geq L$ where v is the y-displacement.

The solution to this problem can be obtained using complex variable methods - see Muskhelishvili's book. For arbitrary values of s there will be unbounded values of $\sigma_{yy}(x, 0)$ as $|x| \to L$ from outside the strip. Only for one value of s will the stresses be bounded as $|x| \to L$. That choice is

$$\frac{s}{L} = 2\sin^2\left(\frac{\pi}{4}\frac{\sigma^\infty}{\sigma_0}\right) \quad \text{or} \quad \frac{s}{a} = \sec\left(\frac{\pi}{2}\frac{\sigma^\infty}{\sigma_0}\right) - 1 \tag{9.1}$$

and this leads to a stress distribution ahead of the crack-tip as shown on the right in Fig. (9.2). With this choice the crack-tip opening displacement (COD or sometimes CTOD) is

$$\delta_t \equiv v(a, 0^+) - v(a, 0^-) = \frac{8}{\pi}\varepsilon_0\, a\ell n\left[\sec\left(\frac{\pi}{2}\frac{\sigma^\infty}{\sigma_0}\right)\right] \tag{9.2}$$

where $\varepsilon_0 = \sigma_0/E$ is essentially the yield strain. See Fig. (9.3) for δ_t . Next we evaluate J using the line integral
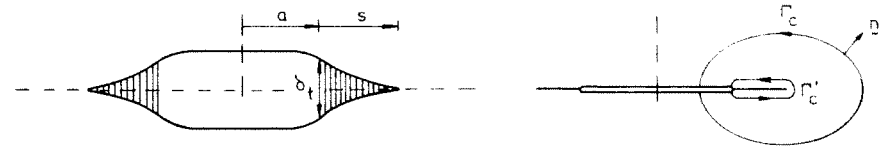
Fig. (9.3).

expression (8.14), where Γ_c is any contour such as that shown in Fig. (9.3). Using the path-independence of J shrink Γ_c to Γ_c' running just along top and bottom of strip zone from $a \leq x \leq L$. Since $n_x = 0$ along Γ_c' and $\sigma_{ij}n_j u_{i,x} = \sigma_0 v_{,x} n_y$, we find

$$J = -\int_{\Gamma_c'} \sigma_0 v_{,x} n_y ds = -\sigma_0 \int_a^L [v_{,x}(x, 0^+) - v_{,x}(x, 0^-)]dx$$

$$= \sigma_0[v(a, 0^+) - v(a, 0^-)] = \sigma_0 \delta_t \tag{9.3}$$

or

$$J = \frac{8}{\pi}\sigma_0\varepsilon_0\, a\ell n\left[\sec\left(\frac{\pi}{2}\frac{\sigma^\infty}{\sigma_0}\right)\right] \tag{9.4}$$

Eq. (9.4) applies only to the finite crack in the infinite plane but (9.3), i.e.

$$J = \sigma_0 \delta_t , \tag{9.5}$$

holds for all configurations for the Dugdale-Barenblatt model. The energy release rate J for the elastic material outside the strip of yielding balances the work-rate of the cohesive stresses $(\sigma_{yy} = \sigma_0)$ applied along the strip.

In s.s.y. when $\sigma^\infty/\sigma_0 \ll 1$, (9.1), (9.2) and (9.3) give

$$\frac{s}{a} = \frac{\pi^2}{8}\left(\frac{\sigma^\infty}{\sigma_0}\right)^2 , \quad J = \sigma_0\delta_t = \pi\sigma_0\varepsilon_0 a\left(\frac{\sigma^\infty}{\sigma_0}\right)^2 \tag{9.6}$$

Recalling $K = \sqrt{\pi a}\,\sigma^\infty$ in s.s.y. these can also be written as

$$s = (\pi/8)(K/\sigma_0)^2 \quad , \quad J = \sigma_0 \delta_t = K^2/E \tag{9.7}$$

which gives results listed earlier.

Denoting the value of J in (9.6) by $(J)_{s.s.y.}$, we can write the l.s.y. result as

$$\frac{J}{(J)_{s.s.y.}} = \frac{8}{\pi^2}\left(\frac{\sigma_0}{\sigma^\infty}\right)^2 \ell n\left[\sec\left(\frac{\pi}{2}\frac{\sigma^\infty}{\sigma_0}\right)\right] \tag{9.8}$$

$$= 1 + \frac{\pi^2}{24}\left(\frac{\sigma^\infty}{\sigma_0}\right)^2 + \ldots \tag{9.9}$$

Thus for $\sigma^\infty/\sigma_0 = 1/2$ the s.s.y. result underestimates J (and δ_t) by about 10%. Note that the ratio (9.7) becomes unbounded as $\sigma^\infty \to \sigma_0$.

One approximate way which has been used for extending s.s.y. results to intermediate scale yielding is based on the concept of an increased effective crack length to account for the plastic zone. The idea is to use the elastic results with a replaced by a_e . The s.s.y. relations are used to define a_e and K_e in terms of J , i.e.

$$J = K_e^2/E \quad \text{and} \quad K_e = \sqrt{\pi a_e}\,\sigma^\infty \quad , \tag{9.10}$$

From (9.9) it follows that

$$K_e^2 = \pi a(\sigma^\infty)^2\left[1 + \pi^2(\sigma^\infty/\sigma_0)^2/24 + \ldots\right]$$

Thus from the definition of a_e in (9.10) we find that to lowest order of correction

$$a_e = a\left[1 + \pi^2(\sigma^\infty/\sigma_0)^2/24 + \ldots\right] = a + s/3 + \ldots \tag{9.11}$$

where s is given by the s.s.y. result (9.6) or (9.7). This approach will be discussed again at a later point in the notes; here we simply remark that the correction $s/3$ in (9.11), which is asymptotically correct for the problem under consideration, is somewhat less than the $s/2$ usually recommended

for plane stress problems.

With (9.2) and (9.4) in hand, we can now discuss a possible extension of the analysis of <u>fracture initiation</u> into the l.s.y. range, at least within the context of the Dugdale model. First note from (9.5) than any criterion based on a critical value of J will necessarily be equivalent to one based on a critical value of δ_t . The COD , δ_t , is a measure of the opening or stretch deep in the plastic zone at the crack tip. The most obvious criterion for initiation which would be independent of whether or not s.s.y. holds is

$$\delta_t = \delta_t^C \tag{9.12}$$

where δ_t^C is to be experimentally determined (as a function of temperature) using some appropriate test specimen. By (9.5), a mathematically equivalent criterion is

$$J = J_C \quad \text{where} \quad J_C = \sigma_0 \delta_t^C \tag{9.13}$$

Under s.s.y. conditions the above can be written in terms of K , using (9.7), as

$$K = K_C \quad \text{where} \quad K_C \equiv \sqrt{\sigma_0 E \delta_t^C} = \sqrt{EJ_C} \tag{9.14}$$

Or, conversely, if K_C is known from a s.s.y. test, then the second equation in (9.14) can be used to define δ_t^C for use in (9.12) or (9.13).

Using (9.4), with $J = J_C$, the stress at initiation σ_C^∞ must satisfy

$$\frac{8}{\pi}\ell n\left[\sec\left(\frac{\pi}{2}\frac{\sigma_C^\infty}{\sigma_0}\right)\right] = \frac{J_C}{\sigma_0 \varepsilon_0 a} \tag{9.15}$$

while using just the s.s.y. formulation (9.14) gives

$$\pi(\sigma_C^\infty/\sigma_0)^2 = J_C/(\sigma_0 \varepsilon_0 a) \tag{9.16}$$

The difference between the predictions (9.15) and (9.16) are

seen in the sketch of σ_c^∞ vs. $1/a$ in Fig. (9.4) where $J_c/(\sigma_0 \varepsilon_0)$ should be regarded as a material constant.
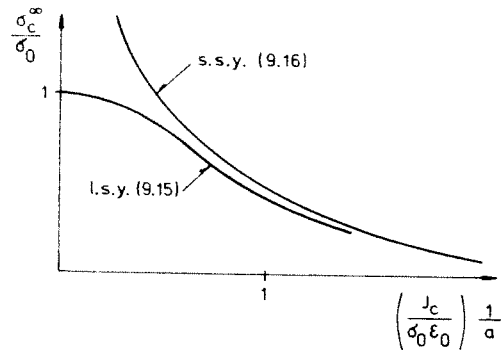
Fig. (9.4).

Dugdale was primarily concerned with estimating the size of the plastic zone in sheets of mild steel. He obtained excellent agreement between the l.s.y. results for s in (9.1) and his experimental observations for applied stress levels approaching the yield stress.

10. CRACK TIP FIELDS

References: J.R. Rice in Fracture, Vol. 2, Section IV, 1971.

J. Hutchinson, J. Mech. Phys. Solids, 16, 13, 337, 1968.

Rice & Rosengren, J. Mech. Phys. Solids, 16, 1, 1968.

Within the context of the small strain deformation theory of plasticity introduced in Section 8 we now investigate the stress and strain fields at the tip of a line crack within the plastic zone. For definiteness consider J_2-deformation theory where

Fig. (10.1).

$$\sigma_e^2 = 3J_2 = \frac{3}{2} s_{ij} s_{ij} \qquad (10.1)$$

where s is the stress deviator and the effective stress reduces to the uniaxial stress in pure tension. Let σ_0 be an effective tensile yield stress (or a reference stress) and let $\varepsilon_0 = \sigma_0/E$ be the associated tensile strain. In tension assume that for $\varepsilon \gg \varepsilon_0$ there is a power-law relation of the form

$$\varepsilon/\varepsilon_0 \sim \alpha(\sigma/\sigma_0)^n \qquad (10.2)$$

where α is a constant. If desired this can be thought of as the plastic part of the strains. Using J_2-deformation theory the above generalizes to

$$\varepsilon_{ij}/\varepsilon_0 \sim \frac{3}{2} \alpha(\sigma_e/\sigma_0)^{n-1} s_{ij}/\sigma_0 \qquad (10.3)$$

Using the line integral expression (8.14) for J, take Γ_c to be a circle of radius r centered at the tip as shown in Fig. (10.1) so that
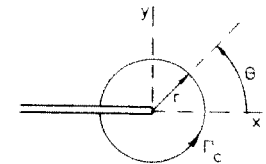
$$J = \int_{-\pi}^{\pi} (Wn_x - \sigma_{ij}n_j u_{i,x})r\,d\theta \qquad (10.4)$$

Since J is independent of the path, r can be chosen to be as small as desired. If J in (10.4) is to have a finite non-zero value as $r \to 0$ it is necessary that

$$\lim_{r \to 0} (Wn_x - \sigma_{ij}n_j u_{i,x})r = f(\theta)$$

or

$$Wn_x - \sigma_{ij}n_j u_{i,x} \sim \frac{f(\theta)}{r} \quad \text{as} \quad r \to 0 \qquad (10.5)$$

Note that the left hand side of (10.5) is homogeneous of degree $(n+1)/n$ in the displacement gradients from (10.2). This suggests that for $r \to 0$

$$W \sim \tilde{W}(\theta)r^{-1} \quad , \quad u \sim \tilde{u}(\theta)r^{\frac{1}{n+1}} \quad , \quad \sigma \sim \tilde{\sigma}(\theta)r^{-\frac{1}{n+1}}$$

The separated form of the dominant singular solution suggested by the above argument has been verified for the power law material by Hutchinson and by Rice and Rosengren. Numerical results for the θ-variations have been obtained and will be displayed below.

The singularity fields can be written as

$$[\sigma_{ij}, \sigma_e] = \sigma_0 K_\sigma r^{-\frac{1}{n+1}} [\tilde{\sigma}_{ij}(\theta, n) , \tilde{\sigma}_e(\theta, n)]$$

$$\varepsilon_{ij} = \alpha \varepsilon_0 K_\sigma^n r^{-\frac{n}{n+1}} \tilde{\varepsilon}_{ij}(\theta, n) \qquad (10.6)$$

$$u_i - u_i^o = \alpha \varepsilon_0 K_\sigma^n r^{\frac{1}{n+1}} \tilde{u}_i(\theta, n)$$

Here the plastic intensity factor K_σ is defined such that K_σ^{n+1} has dimensions of length and its magnitude is specified by normalizing $\tilde{\sigma}_e$ to have a maximum value of unity on the

range $|\theta| \leq \pi$. The dimensionless fields $\tilde{\sigma}_{ij}$, $\tilde{\varepsilon}_{ij}$ and $\tilde{u}_i$ depend on whether Mode I or II pertains, on n , and, most importantly, on whether plane stress or plane strain holds in the plastic zone. The θ-variations of the stress and strain fields for Mode I are shown in Figs. (10.2) and (10.3) for plane stress and in Figs. (10.4) and (10.5) for plane strain. Included are the limiting slip line solutions and associated stress distributions for the perfectly plastic limit $n \to \infty$. Implications of these fields will be discussed in later sections. Here we just take note of the fact that triaxial tension, $\frac{1}{3}\sigma_{kk}$, is highly elevated ahead of the crack in plane strain. For the perfectly plastic limits in Figs. (10.3) and (10.5) one has for $\theta = 0$

$$\sigma_{kk} = \sqrt{3}\,\sigma_0 \qquad \text{in plane stress} \qquad (10.7)$$

$$\sigma_{kk} = \sqrt{3}(1 + \tfrac{1}{2}\pi)\sigma_0 \quad \text{in plane strain} \qquad (10.8)$$

If (10.6) is substituted into the expression (10.4) for J one obtains

$$J = \alpha \sigma_0 \varepsilon_0 K_\sigma^{n+1} I_n \qquad (10.9)$$

where

$$I_n = \int_{-\pi}^{\pi} \left[\frac{n}{n+1} \tilde{\sigma}_e^{n+1} + (\ ) \right] d\theta$$

The complete expression for I_n along with its numerical values are given in Hutchinson, 1968, and also in C.F. Shih, ASTM STP 560, pg. 187, 1974. (For plane stress I_n decreases monotonically from about 5 for $n = 1$ to about 3 for $n \to \infty$, while in plane strain it decreases from about 6 to 4). Using (10.9) we can rewrite (10.6) in a form which emphasises the role of J as a measure of the intensity of the singular crack tip fields:
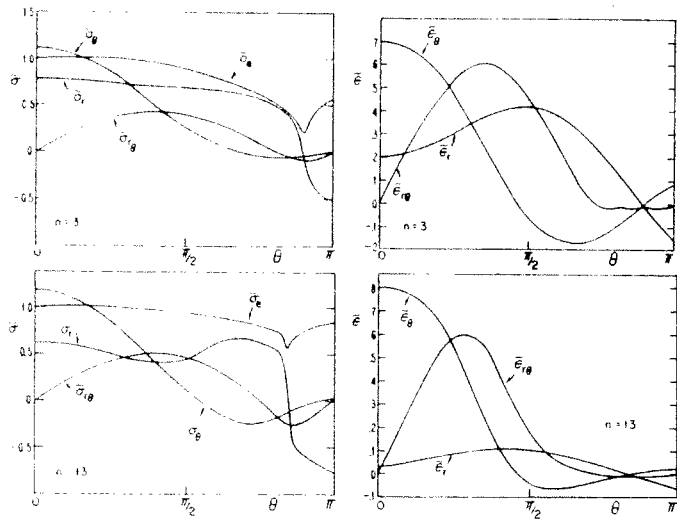
θ-Variation of stresses and strains at the tip of a tensile crack for plane stress.

Fig. (10.2).
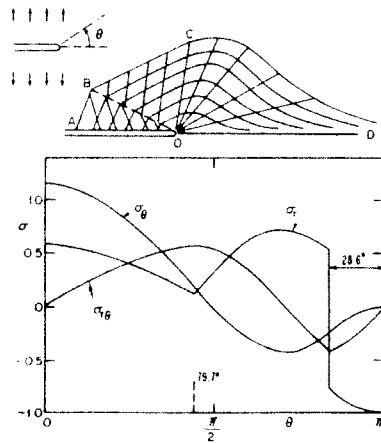
Stress characteristics and stress distribution at the tip of a tensile crack in a perfectly plastic material for plane stress.

Fig. (10.3).
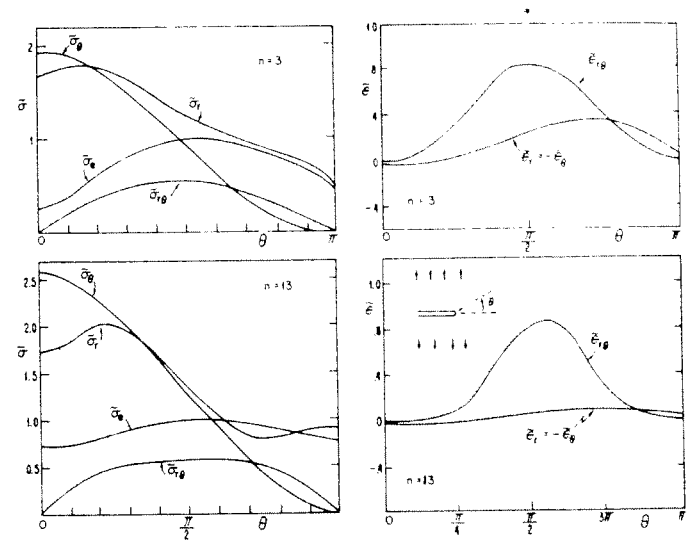
θ-Variations of stress and strains at the tip of a tensile crack for plane strain.

Fig. (10.4).
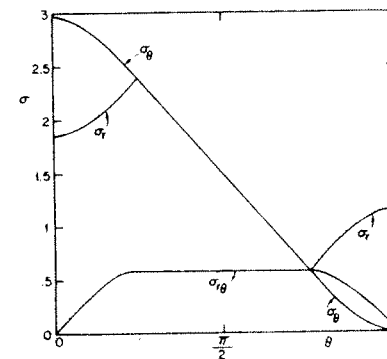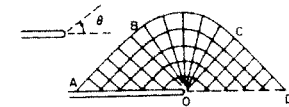
Stress characteristics and stress distribution at tip of a tensile crack in a perfectly plastic material for plane strain.

Fig. (10.5).

$$[\sigma_{ij} , \sigma_e] = \sigma_0 \left(\frac{J}{\alpha \sigma_0 \epsilon_0 I_n r}\right)^{\frac{1}{n+1}} [\tilde{\sigma}_{ij}(\theta , n) , \sigma_e(\theta , n)]$$

(10.10)

$$\epsilon_{ij} = \alpha \epsilon_0 \left(\frac{J}{\alpha \sigma_0 \epsilon_0 I_n r}\right)^{\frac{n}{n+1}} \tilde{\epsilon}_{ij}(\theta , n)$$

The analogous fields in Mode III can be obtained analytically and will appear later in the notes.

We note in passing that the fields (10.10) also hold at the tip of a crack in a material undergoing steady power-law creep. If the ϵ - quantities in (10.2) and (10.3) are identified with the creep strain-rate, as in Norton's law, and if W and u_i in (10.4) are the strain-rate potential and velocity, respectively, then the analysis leading to (10.10) applies rigorously to steady-state creep conditions in which the stresses are unchanging with time. Begley and Landes (ASTM STP 590, pg. 128, 1976) denote the integral (10.4) by J^* (it now has dimensions of stress × length/time) and have used it to correlate creep crack growth data.

We introduced J as an energy-release rate and now find, by virtue of (10.9) or (10.10), that it can also be considered a measure of the intensity of the singular crack tip fields. This is exactly analogous to our earlier reinterpretation of G via its connection with K in linear elasticity. Note that (10.10) reduces to the square root singularity encountered previously for $n = 1$. (The normalization of K_σ in (10.6) for $n = 1$ is different from the way K is normalized in linear elasticity; but (10.10) does reduce to the analogous linear elastic expressions for $\nu = \frac{1}{2}$ corresponding to incompressibility assumed in (10.3)). The local analysis leading to the above crack tip fields (10.10) has not involved any assumption with regard to the extent of plastic yielding and is certainly not confined to s.s.y. In principle, assuming deformation theory supplies an adequate plasticity description under monotonic loading, J provides a unique intensity measure for characterizing fracture initia-

tion at the crack tip under small or large scale yielding conditions. We will discuss the adequacy of deformation theory at a later point of the notes. Here it can simply be noted that the singularity fields themselves under increasing J correspond to proportional loading and therefore the fields (10.10) are also exact solutions to J_2 flow (incremental) theory specialized to the tensile relation (10.2).

The above interpretation of J as an intensity measure, as opposed to the energy release rate of a crack in a fictitious deformation theory solid, provides the theoretical basis for its central role in nonlinear fracture mechanics. Later sections of the notes will discuss experimentation in l.s.y. based on J . Limitations of the approach will also be discussed. The main limitation concerns the size of region over which the singularity fields (10.10) dominate (i.e. accurately predict) the true behavior. It is essential that the region of dominance be large compared to the region in which the microscopic fracture processes are occuring (the fracture process zone) and/or large compared to the region in which the small strain plasticity approximation breaks down. This issue is currently under intensive investigation. It is already possible in this section to give some hint as to how the limitation arise.

The normalized θ - variations $\tilde{\sigma}_{ij}$ and $\tilde{\epsilon}_{ij}$ in (10.10) are unique for finite n . Thus for sufficiently small r J does provide a unique measure of the crack tip fields within the context of the small strain deformation theory. For $n \to \infty$ the stress fields $\tilde{\sigma}_{ij}$ approach the stress fields of the perfectly plastic slip line solutions shown in Figures (10.3) and (10.5). On the other hand, starting from these stress fields for perfect plasticity one can show that the θ - variations of the singular strain fields are not unique but depend on the solution to the entire boundary value problem. (This is a consequence of the fact that the field equations of perfect plasticity are hyperbolic while those for n finite are elliptic).

The singularity of the strains is like $1/r$, as implied

by (10.10) for $n \to \infty$, but the θ - variations cannot be determined from a local analysis (see, eg., Rice, 1971, pg. 267, for a discussion of s.s.y. plane strain). In fact even the stress state at the crack tip is not unique under l.s.y. in perfect plasticity, as will be discussed in more detail later. Under fully yielded conditions the stress and strains fields at the crack tip in a perfectly plastic (Hencky) material are a strong function of the external geometry, particularly in plane strain, in addition to J as emphasised by Mc Clintock (in Fracture, Vol. 3, pg. 48, 1971). Thus to argue that J (or any other parameter) is a unique, configuration-independent, measure of crack tip deformation we must appeal to some strain hardening. At the same time, the present discussion indicates that even with strain hardening the size of the zone of dominance is of some importance and may severely limit range of applicability of J .

11. ELASTIC-PLASTIC SOLUTIONS IN S.S.Y.

References: J.A. Hult and F.A. Mc Clintock, in Proc. 9th Int.
Cong. Appl. Mech., Brussels, 8, pg. 51, 1956.
J. Rice in Fracture, Vol. 2, pg. 246, 1971.
C.F. Shih, ASTM STP 590, pg. 3, 1976.

We digress from our objective of developing l.s.y. fracture mechanics to present in this section some additional details of elastic-plastic solutions in s.s.y. To start we give the solution of Hult and Mc Clintock for a Mode III crack in an elastic-perfectly plastic material.

The solution is exceptionally simple. As sketched in Fig. (11.1) the plastic zone is circular in shape, perched directly at the tip of the crack. Outside the elastic-plastic boundary the solution is just the K-field of the elastic solution but centered at $\bar{r} = 0$ not $r = 0$. Inside the boundary the strains vary everywhere like $1/r$. A quick derivation of the solution will now be given. We will assume deformation
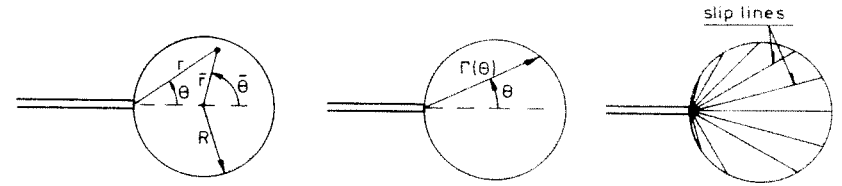
Fig. (11.1).

theory (Hencky theory) but we will show that the solution also satisfies the corresponding flow theory equations.

With K as the Mode III stress intensity factor, the elastic crack-tip fields are (centered at $\bar{r} = 0$)

$$(\tau_{\bar{r}} , \tau_{\bar{\theta}}) = G(\gamma_{\bar{r}} , \gamma_{\bar{\theta}}) = \frac{K}{\sqrt{2\pi\bar{r}}} (\sin\tfrac{1}{2}\bar{\theta} , \cos\tfrac{1}{2}\bar{\theta})$$

(11.1)

$$w = \frac{K}{G} \sqrt{\frac{2\bar{r}}{\pi}} \sin\tfrac{1}{2}\bar{\theta}$$

where $\tau_{\bar{r}} \equiv \sigma_{\bar{r}z}$, $\tau_{\bar{\theta}} = \sigma_{\bar{\theta}z}$, etc.

Inside the plastic zone the following equations must be satisfied (now using a planar polar coordinate system centered at $r = 0$):

$$r^{-1}(r\tau_r)_{,r} + r^{-1}\tau_{\theta,\theta} = 0 \qquad \text{(equilibrium)} \quad (11.2)$$

$$\tau_r^2 + \tau_\theta^2 = \tau_0^2 \qquad \text{(Mises or Tresca yield condition)} \quad (11.3)$$

$$(\gamma_r^e , \gamma_\theta^e) = G^{-1}(\tau_r , \tau_\theta) \qquad \text{(elastic strains)} \quad (11.4)$$

$$(\gamma_r^p , \gamma_\theta^p) = \lambda^p(\tau_r , \tau_\theta) \qquad \text{(plastic strains)} \quad (11.5)$$

$$(\gamma_r , \gamma_\theta) = \lambda(\tau_r , \tau_\theta) \; ; \; \lambda = G^{-1} + \lambda^p \qquad \text{(total strains)} \quad (11.6)$$

$$(\gamma_r , \gamma_\theta) = (w_{,r} , r^{-1}w_{,\theta}) \qquad \text{(strain-displacement)} \quad (11.7)$$

Look for solution of form

$$\tau_r = 0 \ , \ \tau_\theta = \tau_0 \ , \ \gamma_r = 0 \ , \ \gamma_\theta = \lambda(r,\theta)\tau_0 \qquad (11.8)$$

which satisfies (11.2), (11.3) and (11.6). (This special solution corresponds to the fan of straight slip lines shown on the right in Fig. (11.1)). Now look for displacement field $w(r,\theta)$ consistent with (11.8).

$$\gamma_r = 0 \ \rightarrow \ w_{,r} = 0 \ \rightarrow \ w = F(\theta) \qquad (11.9)$$

$$\gamma_\theta = r^{-1} w_{,\theta} = \lambda\tau_0 \ \rightarrow \ \lambda = F'(\theta)/(\tau_0 r) \qquad (11.10)$$

We now show that we can pick $F(\theta)$ such that the two solutions match on the elastic-plastic boundary $\bar{r} = R$. On $\bar{r} = R$, $\bar{\theta} = 2\theta$; transform (11.1) to (r,θ) axes with result (on $\bar{r} = R$) that (11.1) becomes

$$\tau_r = \gamma_r = 0 \ , \ G\gamma_\theta = \tau_0 = K/\sqrt{2\pi R} \ , \ w = KG^{-1}\sqrt{2R/\pi}\sin\theta \qquad (11.11)$$

Traction (and stresses) will be continuous across $\bar{r} = R$ if

$$\frac{K}{\sqrt{2\pi R}} = \tau_0 \quad \text{or} \quad R = \frac{1}{2\pi}\left(\frac{K}{\tau_0}\right)^2 \qquad (11.12)$$

Continuity of w (and strains) across $\bar{r} = R$ requires

$$F(\theta) = KG^{-1}\sqrt{2R/\pi}\sin\theta = 2R\,\gamma_0\sin\theta \qquad (11.13)$$

where $\gamma_0 \equiv \tau_0/G$. With K increasing monotonically the plastic strains increase proportionally at each point (in fact, $\gamma_r^p = 0$) and thus the solution also exactly satisfies the incremental plasticity formulation based on elastic-perfectly plastic flow theory.

The strains (total) in the plastic zone are

$$\gamma_r = 0 \ , \ \gamma_\theta = \frac{1}{r}F'(\theta) = \frac{K}{G}\frac{1}{r}\sqrt{\frac{2R}{\pi}}\cos\theta = \frac{2\gamma_0 R\cos\theta}{r}$$

Noting that $2R\cos\theta = \Gamma(\theta)$, as in Fig. (11.1),

$$\gamma_\theta = \gamma_0\,\Gamma(\theta)\,r^{-1} \qquad (11.14)$$

and this displays the $1/r$ variation expected from the singularity analysis of section 10. The C.O.D., $w(0,\pi)$ - $w(0,-\pi)$, is

$$\delta_t = F(\pi/2) - F(-\pi/2) = 4R\gamma_0 = \frac{2}{\pi}\gamma_0\left(\frac{K}{\tau_0}\right)^2 \qquad (11.15)$$

since all the finite stretching occurs within the plastic zone (i.e., $|\theta| \le \pi/2$) . Since $J = K^2/2G$ in s.s.y. Mode III, (11.12) and (11.15) can be reexpressed as

$$R = J/(\pi\tau_0\gamma_0) \quad \text{and} \quad \delta_t = (4/\pi)J/\tau_0 \qquad (11.16)$$

Next consider the effect of hardening. With

$$\tau = \sqrt{\tau_r^2 + \tau_\theta^2} \quad \text{and} \quad \gamma = \sqrt{\gamma_r^2 + \gamma_\theta^2} \ ,$$

assume,

$$\left.\begin{array}{ll} \gamma/\gamma_0 = \tau/\tau_0 & \text{for} \ \tau \le \tau_0 \\[2mm] \gamma/\gamma_0 = (\tau/\tau_0)^n & \text{for} \ \tau > \tau_0 \end{array}\right\} \qquad (11.17)$$

where $\tau_0 = G\gamma_0$. The deformation theory relation is

$$\left.\begin{array}{ll} \gamma_\alpha/\gamma_0 = \tau_\alpha/\tau_0 & \text{for} \ \tau \le \tau_0 \ (\alpha = 1,2 \ \text{or} \ r,\theta) \\[2mm] \gamma_\alpha/\gamma_0 = (\tau/\tau_0)^{n-1}\tau_\alpha/\tau_0 & \text{for} \ \tau > \tau_0 \end{array}\right\} \qquad (11.18)$$

The s.s.y. problem can again be solved in closed form (see Rice, 1971, pg. 255). It is again found that the plastic zone is circular with precisely the same radius R given before in (11.12). Now the zone completely engulfs the tip (see Fig. (11.2)) with

$$\beta = \frac{n-1}{n+1} \quad \text{and} \quad r_p = \frac{2n}{n+1} R = \frac{2n}{n+1} \frac{1}{2\pi} \left(\frac{K}{\tau_0}\right)^2 \qquad (11.19)$$
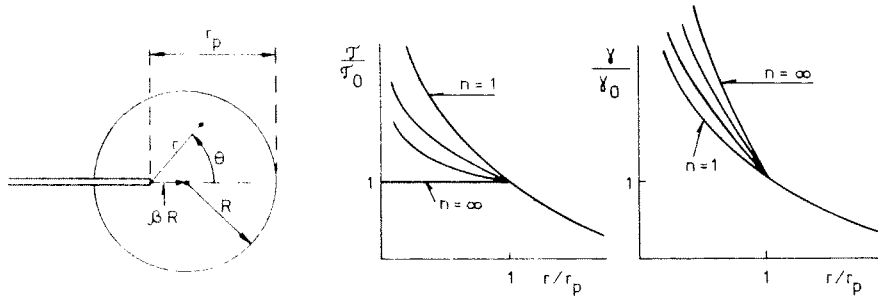

Fig. (11.2).

As in the elastic-perfectly plastic case the dominant singularity is the full solution everywhere within the plastic zone. (This appears to be peculiar to Mode III s.s.y. It is definitely not the case in plane stress or in plane strain or even in s.s.y. Mode III with other stress-strain curves). The singularity field can be written as

$$\tau_\alpha = \tau_0 (r_p/r)^{\frac{1}{n+1}} \tilde{\tau}_\alpha(\theta) \quad , \quad \gamma_\alpha = \gamma_0 (r_p/r)^{\frac{n}{n+1}} \tilde{\gamma}_\alpha(\theta) \qquad (11.20)$$

where

$$[\tilde{\tau}_x(\theta) \ , \ \tilde{\tau}_y(\theta)] = \tilde{\tau}(\theta) \ [-\sin\phi \ , \ \cos\phi]$$

$$[\tilde{\gamma}_x(\theta) \ , \ \tilde{\gamma}_y(\theta)] = \tilde{\tau}^n(\theta) [-\sin\phi \ , \ \cos\phi]$$

$$\tilde{\tau}(\theta) = \left[\frac{n+1}{2n} \frac{\sin 2\phi}{\sin\theta}\right]^{\frac{1}{n+1}} \quad (\text{note: } \tilde{\tau}(0) = 1)$$

and

$$2\phi = \theta + \arcsin\left[\frac{n-1}{n+1} \sin\theta\right] .$$

Sketches of the stress and strain directly ahead of the crack ($\theta = 0$) are shown in Fig. (11.2). From (11.20) they are given by

$$\tau_y = \tau_0 (r_p/r)^{\frac{1}{n+1}} \quad , \quad \gamma_y = \gamma_0 (r_p/r)^{\frac{n}{n+1}} \qquad (11.21)$$

For $n = 1$ and $n \to \infty$ (11.20) and (11.21) reduce to the previously obtained limit of elasticity and perfect plasticity, respectively. The fields (11.20) in the plastic zone display proportional loading so the above solution is again an exact solution to the corresponding incremental field equations.

Closed form solutions for the stresses and strains everywhere in the plastic zone have not been obtained for Mode I or II situations. As already mentioned, the dominant singularity fields are not the full solutions everywhere in the zone. Many finite element studies of the s.s.y. problem in plane strain Mode I have been made. It is generally agreed that the difference between, say, the predictions of J_2 deformation theory and J_2 flow theory are of little consequence. For example, evaluation of the J integral on many different paths using J_2-flow theory solutions reveals very little path dependence, implying that the deformations satisfy nearly proportional loading.

Boundaries of the plastic zone in s.s.y. plane strain are shown in Fig. (11.3). This figure is taken from Shih, 1976; it includes four cases ranging from Mode I ($M^e = 1$) to Mode II ($M^e = 0$) where the measure of the combination of mixed modes is

$$M^e = (2/\pi) \tan^{-1} |K_I/K_{II}|$$

A piecewise power-hardening law was used to represent the material in Fig. (11.3) along with J_2 deformation theory, i.e.,

$$\varepsilon = \sigma/E \ , \ \sigma \le \sigma_0 \ ; \ \varepsilon/\varepsilon_0 = (\sigma/\sigma_0)^n \quad \sigma > \sigma_0 \qquad (11.22)$$

In s.s.y. the size of the plastic zone is proportional to

$(K/\sigma_0)^2$ and thus the plots of Fig. (11.3) are independent of K in s.s.y.

In plane stress Mode I the plastic zone shapes and sizes are similar to those in Mode III, as seen in Fig. (4.2) and in equation (4.2).
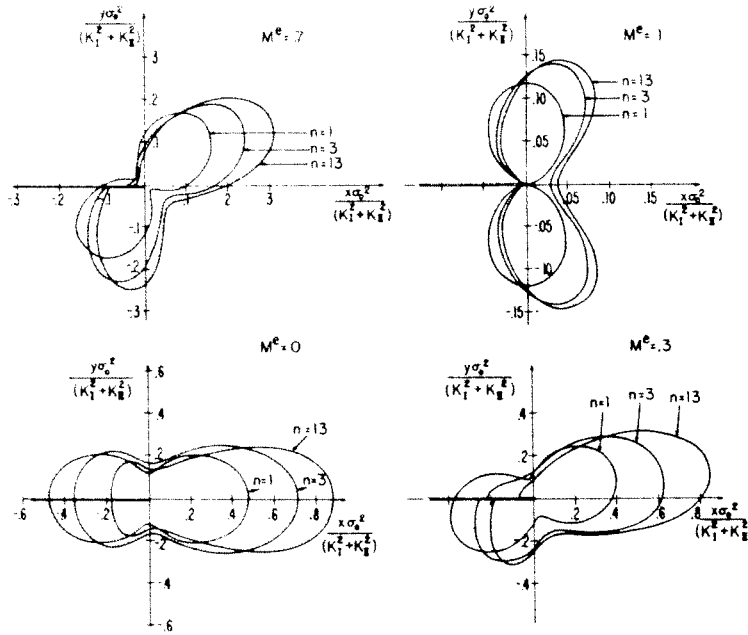
Elastic-plastic boundaries for small-scale yielding in plane strain.

Fig. (11.3).

12. ANALYSIS OF L.S.Y.

In this section we discuss three aspects of large scale yielding analysis: (1) a special, simple expression for J for deeply-cracked bend specimens, (2) plastically adjusted crack lengths for extending s.s.y. results, and (3) estimation procedures using fully plastic power-law solutions. Finite element studies will be discussed later in the notes.

J for deeply-cracked bend specimens

Consider the configuration in Fig. (12.1) where M is the moment/unit thickness applied to the specimen. As on page 26 of the notes, let θ_{nc} denote the load point rotation with a = 0 and θ_{cr} the contribution due to the presence of the crack such that the total rotation is given by

$$\theta = \theta_{nc} + \theta_{cr} \qquad (12.1)$$

Defined in this way θ_{cr} is independent of L , assuming L is sufficiently large compared to b , and thus, in general,

$$\theta_{cr} = F\left(\frac{M}{\sigma_0 c^2} , \frac{c}{b} , \frac{\sigma_0}{E} , n , etc. \right) \qquad (12.2)$$

Here, F is dimensionless, σ_0 is some appropriately defined yield stress, and F may be a function of additional non-dimensional groups of material characterizing parameters.
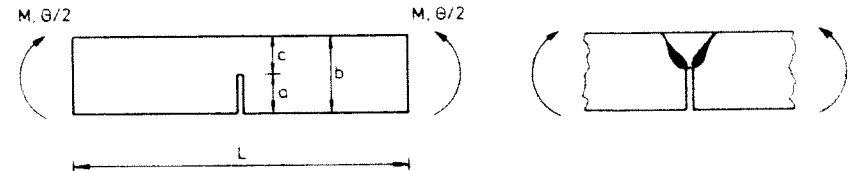
Fig. (12.1).

For cracks which are sufficiently deep, i.e. $c/b \ll 1$, F will be independent of c/b. For example in the linear elastic range, from (6.20),

$$\theta_{cr} = 16M/(\bar{E}c^2) \quad \text{as} \quad c/b \to 0 \tag{12.3}$$

In the fully yielded range plasticity will be confined to the area of the uncracked ligament as depicted in Fig. (12.1) and then it is clear that b does not enter in (12.2).

Next, convert the general expression for J in (8.9) to the present case noting $\partial\theta/\partial a = \partial\theta_{cr}/\partial a$

$$J = \int_0^M \frac{\partial\theta_{cr}}{\partial a} (\tilde{M}, a) d\tilde{M} \tag{12.4}$$

From (12.2),

$$\left(\frac{\partial\theta_{cr}}{\partial a}\right)_M = -\left(\frac{\partial\theta_{cr}}{\partial c}\right)_M = 2F_{,1}\frac{M}{\sigma_0 c^3} - F_{,2}\frac{1}{b} \tag{12.5}$$

where the commas denote the obvious partial derivatives. Next note that

$$\left(\frac{\partial\theta_{cr}}{\partial M}\right)_a = F_{,1}\frac{1}{\sigma_0 c^2}$$

so that (12.5) can be rewritten as

$$\left(\frac{\partial\theta_{cr}}{\partial a}\right)_M = \left(\frac{\partial\theta_{cr}}{\partial M}\right)_a \frac{2M}{c} - F_{,2}\frac{1}{b} \tag{12.6}$$

Now substitute (12.6) into (12.4) noting that $(\partial\theta_{cr}/\partial M)_a dM = d\theta_{cr}$ (with a held fixed) with the result

$$J = \frac{2}{c}\int_0^M M d\theta_{cr} - \frac{1}{w}\int_0^M F_{,2} dM \tag{12.7}$$

When the specimen is deeply cracked $F_{,2} \approx 0$, as already discussed, and (12.7) reduces to

$$J = \frac{2}{c}\int_0^M M d\theta_{cr} \tag{12.8}$$

This is the expression of Rice, Paris and Merkle (ASTM STP 536, 1973). It has the simple interpretation of $(2/c)$ times the area under the M vs. θ_{cr} curve. This relation can be measured experimentally in any test, and thus (12.8) permits J to be determined directly from the experimental record, as long as there is no appreciable crack growth. The derivation given above leading to (12.7) is due to P.C. Paris (unpublished) and includes the general form of the correction term to account for finite values of c/b. It is felt, that (12.8) provides a reasonably good approximation as long as $c/b \leq 1/2$, although more work is needed to tie this down.
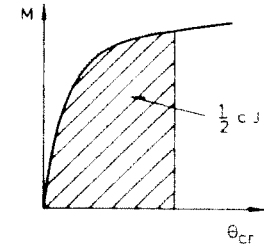
Fig. (12.2).

Similar reductions of J are possible for other deeply-cracked configurations as can be found in the paper by Rice, Paris and Merkle.

Plastically adjusted crack lengths

In connection with the Dugdale model in Section 9 it was seen that it is possible to extend the range of s.s.y. somewhat by using the idea of a plastically adjusted crack length a_e in the s.s.y. (i.e. elastic) formulas. The standard proposal (see, for example, Tada, Paris and Irwin, 1973, pg. 1.17) is that $a_e = a + r_y$ where (cf. pg. 14 of notes)

$$r_y = \frac{1}{2}r_p = (1/2\pi)(K/\sigma_0)^2 \quad \text{in plane stress} \tag{12.9}$$

$$r_y = \frac{1}{2}r_p = (1/6\pi)(K/\sigma_0)^2 \quad \text{in plane strain} \tag{12.10}$$

For the Dugdale model we have seen that the asymptotically correct adjustment is $r_y = \frac{1}{3}r_p$, at least for the finite crack in the infinite sheet. Edmunds and Willis (J.M.P.S. 1976, 24, 205 and 225, and 1977, 25, 423) have shown that

$$r_y = 1/3 r_p = (\pi/24)(K/\sigma_0)^2 \qquad (12.11)$$

provides an asymptotic correction for all configurations for the Dugdale model.

For Mode III crack problems where the material satisfies (11.17) and (11.18) Edmunds and Willis have shown that the asymptotic correction should be (see Fig. (11.2))

$$r_y = \frac{n-1}{n+1} R = \frac{1}{2\pi}\left(\frac{n-1}{n+1}\right)\left(\frac{K}{\tau_0}\right)^2 \qquad (12.12)$$

as suggested by the analysis of Section 11. For Mode I plane strain Edmunds and Willis find that the universal correction for elastic-perfectly plastic materials satisfying the Mises yield condition is

$$r_y = .019(K/\sigma_0)^2 \qquad (12.13)$$

and this is about 1/3 the commonly used value (12.10). The corresponding calculation for plane stress has not been performed but, judging from Mode III, (12.9) should not be far off.

Edmunds and Willis show how the asymptotic expansion can be continued to higher order terms. The corrections beyond the plastic adjustment inherently involve details of the overall geometry and loading beyond that supplied by the elastic K.

To summarize, if $K = f(a)P$ denotes the stress intensity factor for a crack of length a from the elastic solution. Then, with $a_e = a + r_y$, the adjusted value of K is $K_e = f(a_e)P$ and the J value from the s.s.y. formula is

$$J = K_e^2/\bar{E} \qquad (12.14)$$

The extension of the range acheived by this approach is not necessarily very large. For the Dugdale problem considered in Section 9 (see Edmunds and Willis, 1977, pg. 436, figure 4) J is given to within 10% for σ^∞/σ_0 up to about .7 as opposed to .5 without the correction. It is possible that the plane

strain correction (12.10) gives a better approximation than (12.13) over a more extended range even though (12.13) is asymptotically correct. This is an open question.

Fully plastic solutions and l.s.y. estimates

First we consider a class of small strain fully plastic crack problems in which the "elastic" strains are neglected and the tensile behavior is governed by

$$\varepsilon/\varepsilon_0 = \alpha(\sigma/\sigma_0)^n \qquad (12.15)$$

Using J_2 deformation theory with $\sigma_e^2 = (3/2)s_{ij}s_{ij}$

$$\varepsilon_{ij}/\varepsilon_0 = (3/2)\alpha(\sigma_e/\sigma_0)^{n-1}s_{ij}/\sigma_0 \qquad (12.16)$$

As noted by Ilyushin many years ago, a solution to a boundary value problem involving a single load or displacement parameter which is increased monotonically has two important properties. If P is a load parameter then stresses increase in direct proportion to P while strains increase as P^n. Since the stressing is proportional at every point the solution based on (12.16) is also an exact solution to corresponding flow theory problem. It should also be noted that with ε_{ij} identified with the strain-rate the solution will also be a solution for steady power law creep.

Because of the pure-power behavior the load dependence of the solution factors out trivially. For example, J is necessarily proportional to P^{n+1}. To illustrate the simple form the solutions take consider the strip of Fig. (12.1) in bending in either plane strain or plane stress. Defining θ_{cr} as in (12.1) and assuming L is sufficiently long such that the dependence of θ_{cr} on L is negligible, we can write

$$J = \alpha\sigma_0\varepsilon_0 c\, h_1(a/b\,,\,n)(M/M_0)^{n+1} \qquad (12.17)$$

$$\theta_{cr} = \alpha\varepsilon_0 h_3(a/b\,,\,n)(M/M_0)^n \qquad (12.18)$$

where M_0 is a reference moment/unit thickness quantity. The most convenient choice for M_0 is the limit moment of a perfectly plastic $(n \to \infty)$ material. Assuming that a is not too small, this choice is

$$M_0 = A \sigma_0 c^2 \qquad (12.19)$$

where $A = .364$ in plane strain and $A = .268$ in plane stress. For given values of a/b and n, h_1 and h_3 can be calculated once and for all using finite element methods. Solutions to a number of fully plastic problems are now available. A list of references is given by Hutchinson, Needleman and Shih (1978, Harvard University Report Mech-6 to be published in O.N.R. Symposium on Fracture Mechanics, Washington, D.C.). For the strip in bending numerical results from Hutchinson, *et al.* for $a/b = 1/2$ are given in the Table.

	$a/b = 1/2$	$n = 1$	$n = 2$	$n = 3$	$n = 5$	$n = 7$	$n = 10$
plane strain	h_1	1.49	1.33	1.21	1.04	.906	.742
	h_3	2.68	2.51	2.26	1.82	1.51	1.20
plane stress	h_1	1.10	.97	.85	.72	.65	.55
	h_3	2.75	2.36	2.03	1.59	1.37	1.12

Next, we consider using the fully plastic solutions, together with the elastic solutions, to interpolate over the range from s.s.y. to l.s.y. To be specific suppose the tensile behavior of the material is characterized by a Ramberg-Osgood relation of the form

$$\varepsilon/\varepsilon_0 = \sigma/\sigma_0 + \alpha(\sigma/\sigma_0)^n \qquad (12.20)$$

where $\sigma_0 = E \varepsilon_0$. In addition, consider the edge-cracked strip in bending. In the s.s.y. range we expect J and θ_{cr} to be given by the elastic results. With $K = f_1(a)M$, these are denoted by

$$J = K^2/\overline{E} = f_1^2(a)M^2/\overline{E} \quad , \quad \theta_{cr} = f_3(a)M \qquad (12.21)$$

where f_1 and f_3 are known functions from, for example, Tada, *et al.* In the l.s.y. range we expect J and θ_{cr} to approach the values given by (12.17) and (12.18) for the fully plastic solution as M increases.

To interpolate over the entire range Shih and Hutchinson (J. Eng. Mat. and Tech., 98, 1976, pg. 289) have proposed

$$J = f_1^2(a_e)M^2/\overline{E} + \alpha \sigma_0 \varepsilon_0 c\, h_1(a/b , n) (M/M_0)^{n+1} \qquad (12.22)$$

$$\theta_{cr} = f_3(a_e)M + \alpha \varepsilon_0 h_3(a/b , n) (M/M_0)^n \qquad (12.23)$$

Here $a_e = a + r_y$ where for plane stress, from (12.9) (and (12.12)),

$$r_y = \frac{1}{2\pi}\left(\frac{n-1}{n+1}\right)(K/\sigma_0)^2 \qquad M \le M_0$$
$$= (r_y)_{M = M_0} \qquad M > M_0 \qquad (12.24)$$

where in (12.24) K is given by the elastic formula, i.e. $K = f_1(a)M$. It is clear that som plastic adjustment of the elastic part in (12.22) is needed since without it J would be given by the purely elastic result for $M \le M_0$ for the elastic-perfectly plastic limit $n \to \infty$.

Comparisons between the predictions of (12.22) and (12.23) and full finite element calculations are shown in Fig. (12.3) taken from Shih and Hutchinson. These results are for plane stress with $a/b = 1/2$ and $\alpha = 3/7$; the values of h_1 and h_3 are from the Table. The solid line curves are obtained from (12.22) and (12.23), while the dashed line curves are the finite element results. The curves for the elastic case, $n = 1$, are obtained from the s.s.y. formulas, i.e. (12.22) and (12.23) with $a_e = a$ and $\alpha = 0$. The limit for the elastic-perfectly plastic case $n \to \infty$ is the same as the estimate of Bucci, *et al.* (ASTM STP 514, 1972, pg. 40) using results from limit analysis. Equally good comparisons to those
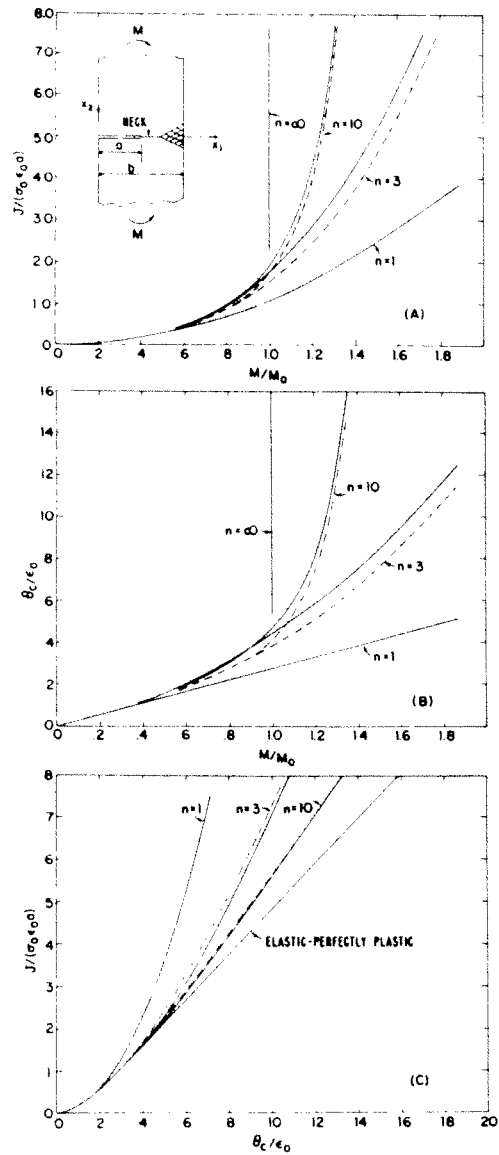
Fig. (12.3).

13. J-INTEGRAL TESTING

References: P.C. Paris, ASTM STP 631, pg. 3, 1977.

Various papers in ASTM STP 590, 1976.

C. Shih, H. de Lorenzi and W. Andrews, "Studies on Crack Initiation and Stable Crack Growth" to be published in an ASTM STP 1978.

Most attention to date has been directed to plane strain testing. This section will be confined to plane strain conditions; application to plane stress conditions is similar in principle.

Test specimens are designed such that a simple formula for J , based on the deeply-cracked assumption, can be used to determine J as a function of load-point displacement directly from the measured load-displacement curve. The expression (12.8) for the strip in bending is one example; with slight modification, this same expression applies to a deeply-cracked compact tension specimen, i.e.

$$ J = (2/c) \int_0^P P \, d\Delta_{cr} \qquad (13.1) $$

where P is the load/unit thickness and c is the uncracked ligament. Corrections to (13.1) accounting for finite values of the ratio of c to specimen width have been proposed by Merkle and Corten (J. Pressure Vessel Tech., 1974, pg. 286) but their status is unclear when l.s.y. occurs. Often Δ_{cr} will be replaced by Δ in (13.1) since Δ_{nc} can usually be neglected in the compact tension specimen.

The current practice is to use (13.1) to determine J up to initiation and also for small amounts of crack growth; the validity of doing this will be discussed later. At the same time, the amount of crack growth Δa is determined by compliance measurements or other techniques. This data is then presented as a cross-plot of J vs. Δa . Some data for a compact tension specimen of A533-B pressure vessel steel at $93^{\circ}C$ are shown in Figures (13.1) through (13.5), taken from

the report of Shih, *et al.* 1978. The specimen from which this data was taken had an initial uncracked ligament c = 86 mm . The steel has an intermediate yield stress of about 500 MN/m^2 and a high toughness of about $J_{IC} \cong$ .2 MJ/m^2 . The resistance curve data of J vs. Δa is obtained from a number of specimens of the same type with varying ligament size. The J_{IC} value is obtained by extrapolating the curve of J vs. Δa back to $\Delta a = 0$ or, sometimes, back to the "blunting" line $J = 2\sigma_0 \Delta a$, which accounts approximately for apparent crack growth due to crack tip blunting.

Initiation in the A533B specimens takes place under fully yielded conditions - see the table on pg. 18 of the notes for an indication of the size requirements for a K_{IC} test. The data in Figs. (13.6) and (13.7) are for a Ni-Cr-Mo steel with a higher yield stress (over 1000 MN/m^2) and a lower fracture toughness ($J_{IC} \approx$ .08 MJ/m^2) . The tests (by J.H. Underwood, Exp. Mech., Sept. 1978, pg. 350) range over bend-type specimens which satisfy the valid K_{IC} testing require-ments to those which involve intermediate scale yielding. This is brought out by the variation of K_{IC} in Fig. (13.7) against the sizing parameter $c\sigma_0/(2.5 \ K_{IC})^2$ - recall eq. (5.5). The determination of K_{IC} in the open points in this figure employed the J-testing technique; K_{IC} is calculated from J_{IC} by

$$K_{IC} = \sqrt{\bar{E} J_{IC}} \qquad (13.2)$$

where $\bar{E} = E/(1 - \nu^2)$. The J_{IC} measurements are consistent with the fracture toughness measurements from valid K_{IC} tests which are denoted by solid points.

The thickness of the specimen must be sufficient to ensure that plane strain conditions prevail everywhere in the yielded zone through most of the thickness. Side groves are sometimes used to reduce the shear tip effects at the lateral surfaces as discussed by Shih, *et al.* It is also essential that the specimen be sized such that all dimensions must be large compared to the region of inherently nonlinear geometric
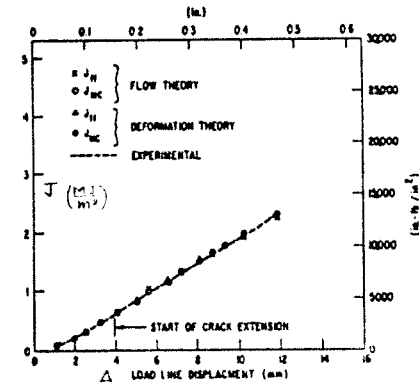
Fig. (13.1). J-integral vs. load-line deflection for specimen T52.
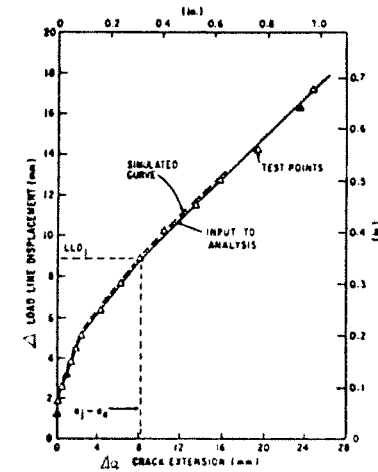
Fig. (13.2). Load-line displace-ment vs. crack extension for 4T compact specimen T52.
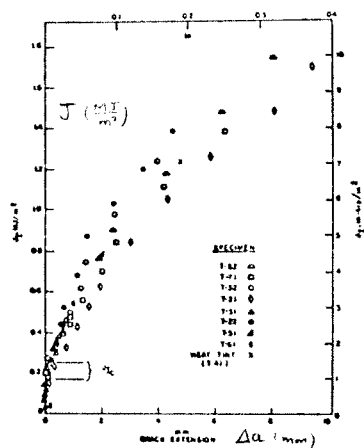
Fig. (13.3). J-resistance curves
for A533B material 2 tested, at
93°C - 4T side-grooved compact
specimens.
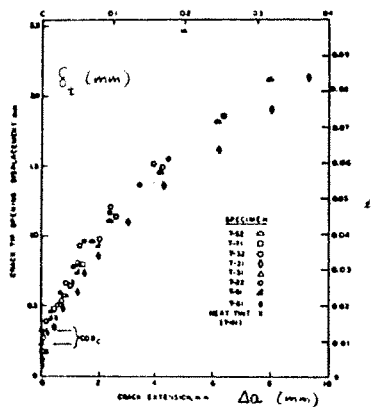
Fig. (13.4). COD-resistance for
A533B material 2, tested at
93°C   T4 side-grooved compact
specimens.
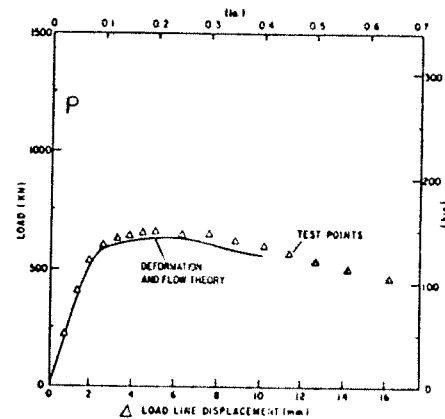
Fig. (13.5). Applied load vs.
load-line displacement for 4T
compact specimen T52, 25% side-
grooved, $(W - a_o) = 86$ mm
(3.385 in.).
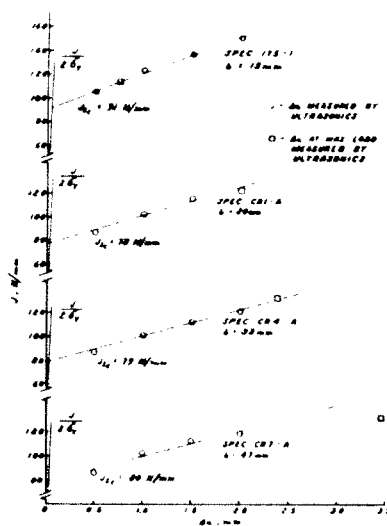
Fig. (13.6). J vs. crack-growth
plots for C-shaped specimens.
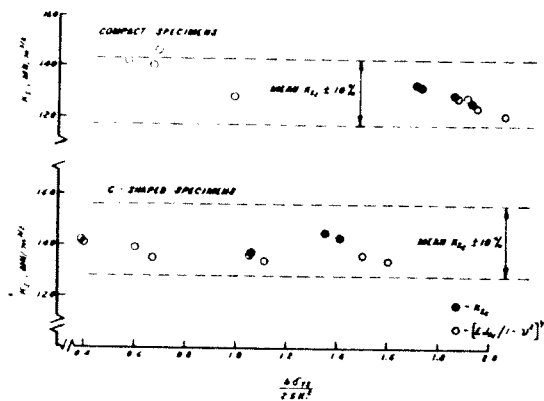
Fig. (13.7). K_{IC} and
$[EJ_{IC} - \nu^2]^{\frac{1}{2}}$ for various
specimen sizes.

behavior. This region is on the order of the crack tip opening displacement, i.e. on the order of J/σ_0 . As discussed by Paris (1977), the requirement for bend-type specimens, which appears to be adequate, is that the thickness and uncracked ligament c both satisfy

$$c \geq 25\, J/\sigma_0 \qquad\qquad (13.3)$$

For center-cracked specimens in tension (13.3) is not adequate, as will be discussed in the next section.

Other studies along these lines can be found in the literature. The general conclusion is that the J-method does give fracture toughness measurements which are in agreement with those obtained from valid K_{IC} tests. Most of the studies have used bend-type specimens, compact tension specimens being considered in this class. Begley and Landes (see, for example, Int. J. of Fracture, 12, pg. 764, 1976) used center-cracked tension specimens as well as bend-type specimens. Their measured values of J_{IC} using the extrapolation method just described gave similar results for the various specimen types. On the other hand the slope of the resistance curve (J vs. Δa) differed by almost a factor of three. Furthermore, the crack in the tension specimens advanced at 45° to the initial plane of the crack, while the crack advanced in the plane in the bend-type specimens. Other tests have found that J_{IC} and δ_t^c measurements using center-cracked specimens in tension are as much as two times the values obtained from bend-type specimens even when (13.3) is satisfied. The reason for this is taken up in the next section.

14. CONFIGURATION DEPENDENCE IN L.S.Y. AND LIMITATIONS OF SINGLE PARAMETER CRACK TIP CHARACTERIZATIONS

References: R.M. McMeeking, J. Mech. Phys. Solids 25, 357, 1977.

R.M. McMeeking and D.M. Parks, "On Criteria for J-Dominance of Crack Tip Fields in L.S.Y.", to be published in ASTM-STP.

C.F. Shih and M.D. German, "Requirements for a One Parameter Characterization of Crack Tip Fields by the HRR Singularity" G.E. Technical Report, Oct. 1978 (to be published).

On pages 47 and 48 of the notes we have already mentioned that the idea of a dominant singularity uniquely tied to J or δ for all configurations involves the assumption of strain hardening. With strainhardening, it is also essential that the size of the region dominated by the singular fields, as determined from the small strain plasticity theory, be large compared to the region of large strains governed by finite strain plasticity. In relatively ductile metals the fracture process zone is comparable in size to this zone of "large" strains.

Slip line fields for three rigid-perfectly plastic plane strain configurations are shown in Figs. (14.1)-(14.3). These and others can be found in the article by McClinock in *Fracture* vol. 3, 1971. (Also displayed there are pictures of actual straining patterns in steel specimens obtained by etching). The near-tip stress field of the edge-cracked strip in tension in Fig. (14.1) is the same found for the limit of the singularity fields as n → ∞ which is shown in Fig. (10.5). This Prandtl field is characterized by the high triaxial stress, σ_{kk} , ahead of the crack (10.8) as well as a high normal stress ahead of the crack. Small scale yielding finite element solutions in plane strain for elastic-perfectly plastic materials give strong support to the attainment of the Prandtl field at the tip of the crack (e.g., D.M. Tracey, J. Engr. Mat.
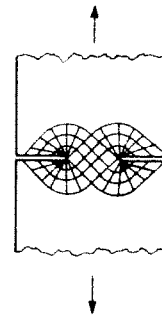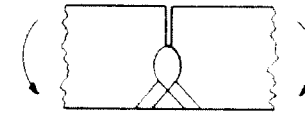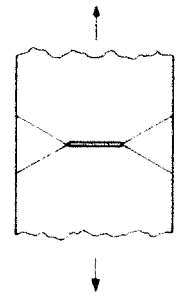
Fig. (14.1).   Fig. (14.2).   Fig. (14.3).

Tech., 98, pg. 146, 1976). For the bend specimen in Fig. (14.2), the singular strains are concentrated along a lens shaped arc. According to the rigid-perfectly plastic solution, the triaxial and normal stresses ahead of the crack do not quite attain the high levels found in s.s.y. or in the edge-cracked strip. However, numerical solutions reported below for elastic-perfectly plastic materials, as well as for strain hardening materials, indicate very little difference near the crack tip between this case and s.s.y. or the edge-cracked strip at corresponding levels of J .

The near-tip behavior for the fully yielded, rigid-perfectly plastic center-cracked strip in Fig. (14.3) is entirely different from the other cases. Here intense shear deformation is confined to slip planes eminating at 45° from the tensile direction. A state of plane strain tension exists ahead of the crack in the 90° wedge where the normal and triaxial stresses are given by

$$\sigma_{yy} = (2/\sqrt{3})\sigma_0 \quad \text{and} \quad \sigma_{kk} = \sqrt{3}\,\sigma_0 \tag{14.1}$$

Thus the stress levels near the crack tip in the rigid-plastic fully yielded center-cracked strip are much below the levels in the other cases. At the same value of J , the strain levels will be correspondingly higher on planes of approximately $\pm 45^\circ$ to the tensile axis eminating from the tip. Thus, the rigid-perfectly plastic solutions for fully yielded specimens

indicate that the crack tip fields are configuration-dependent and cannot be characterized by a single parameter such as J or δ . Strain hardening can substantially alter the rigid-perfectly plastic fields. We now discuss some very recent work, most of which is not yet published, which is directed to determining the conditions for J-dominance of crack tip behavior.

Work of McMeeking (1977) and McMeeking and Parks (1978) based on finite strain, finite element methods has shown that finite strain effects are important over distances of about 2 or 3 times crack opening displacement. In plane strain s.s.y. the crack tip opening displacement δ_t is given by

$$\delta_t = d(\sigma_0/E , n)J/\sigma_0 \qquad (14.2)$$

where the coefficient d is a weak function of σ_0/E and a fairly strong function of n varying from about .6 for very large n to about .3 for $n = 3$. (Detailed results for d will be given later). Beyond 2 or 3 times δ_t the stress and strain fields essentially coincide with the results from a small strain formulation. McMeeking also found that J was essentially path-independent for all contours which fell outside a radius of $3\delta_t$ (a finite strain, J_2 flow theory was used in the calculations).

McMeeking and Parks (1978) calculated the stresses and strains near the crack tip in an edge-cracked bend specimen and in a center-cracked strip in tension from s.s.y. to fully plastic yielding. These they compared with the s.s.y. distributions normalized in a proper way. If the fields are J dominated, plots of stresses and strains near the tip against $r/(J/\sigma_0)$ should be independent of J . This was found to be the case for the bend specimen even with no strain hardening. On the other hand, they found significant deviation from the normalized s.s.y. distributions already in the inter-mediate yielding range for the center-cracked strip. Their results for the center-cracked strip are sketched roughly in Fig. (14.4). Here, for a material with $n = 10$ and
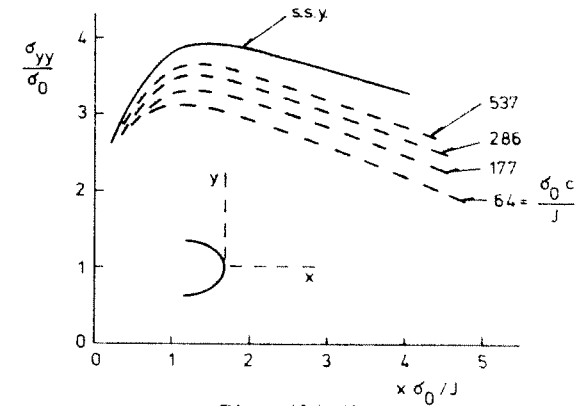
Fig. (14.4).

$\sigma_0/E = 1/300$, the normal stress ahead of the crack is plotted against $x/(J/\sigma_0)$. The solid line is the s.s.y. result. The dashed lines correspond to various levels of intermediate scale yielding as determined by $J/(\sigma_0 c)$ where c is the uncracked ligament. The lowest dashed curve for $\sigma_0 c/J = 64$ corresponds to fully yielded conditions. Similar plots for strains on $45°$ planes indicate an intensification above the normalized s.s.y. results which becomes expecially pronounced for $c\sigma_0/J < 200$. McMeeking and Parks tentatively proposed that the size requirement for the center-cracked strip in tension (plane strain) should be

$$c \geq 200 \ J/\sigma_0 \qquad (14.3)$$

assuming the material does not have high strain hardening. They find that the original proposed (13.3) for bend-type configurations is adequate for essentially any level of strain hardening.

Shih and German (1978) calculated stresses and strains near the crack tip using a finite element method based on a small strain formulation of J_2 flow theory for a deeply-cracked bend specimen (CBB) and a center-cracked strip in tension (CCP), both in plane strain. Employing a normalized plot similar to Fig. (14.4), they compared the calculated stress and strain distributions directly with the HRR singularity

the Shih and German paper. Shown is the normal stress ahead of the crack σ_{yy} at various load levels (eg. values of $c\sigma_0/J$) ranging from essentially s.s.y. to fully plastic yielding. For both $n = 3$ and $n = 10$, the stress distribution (and strain) of the bend specimen is well approximated by the HRR singularity field for distances which are always greater than 2 or 3 times J/σ_0, i.e. always greater than about 4 to 6 times the COD, as long as (13.3) is satisfied. This is not the case for the center-cracked strip (CCP). For the low strain hardening case, $n = 10$, the results of Fig. (14.6) are consistent with the size restriction (14.3). For high strain hardening $(n = 3)$ (14.3) can be relaxed somewhat.

More work is needed to tie down the circumstances under which a single parameter such as J or δ can be used to characterize the crack tip fields. What is clear however is that the restrictions are a strong function of the configuration-type when large scale yielding occurs. The condition (14.3) for center-cracked configurations may effectively mean that the analysis of initiation and growth in this configuration cannot be related to s.s.y. or bend-type data for intermediate strength, high toughness metals. For these materials $200\ J/\sigma_0$ can be on the order of 100 mm at initiation, and this would limit testing and application to very large specimens and cracked bodies. On the other hand, for the other types of configurations it appears as if the weaker requirement (13.3) is adequate to ensure correspondence with s.s.y. data. Furthermore, (13.3) does not seem to be strongly dependent on the level of strain hardening.

Analogous studies in plane stress have not been made. It is possible that the configuration-dependence under fully plastic conditions will not be as strong as in plane strain, primarily because the perfectly plastic limit solutions do not display as wide a variation at least as far as the stresses are concerned.
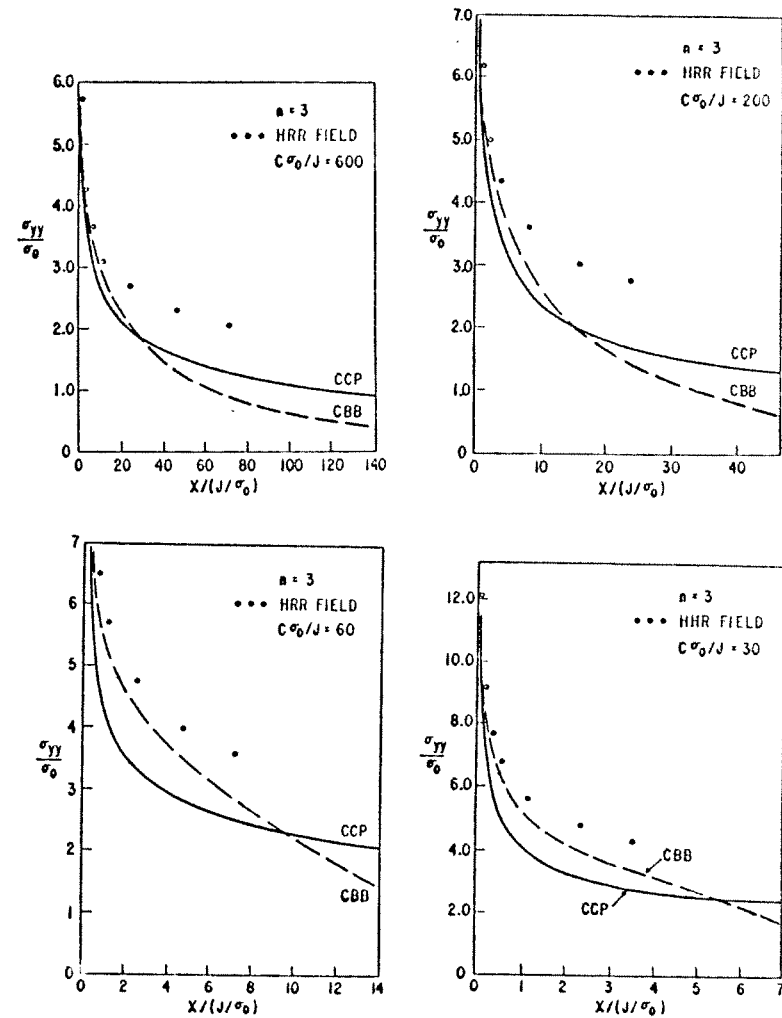
Fig. (14.5). Normal stress ahead of crack in CBB and CCP from obtained to fully plastic conditions with $n = 3$, $\sigma_0/E = 0.002$ and $a/b = 0.75$.
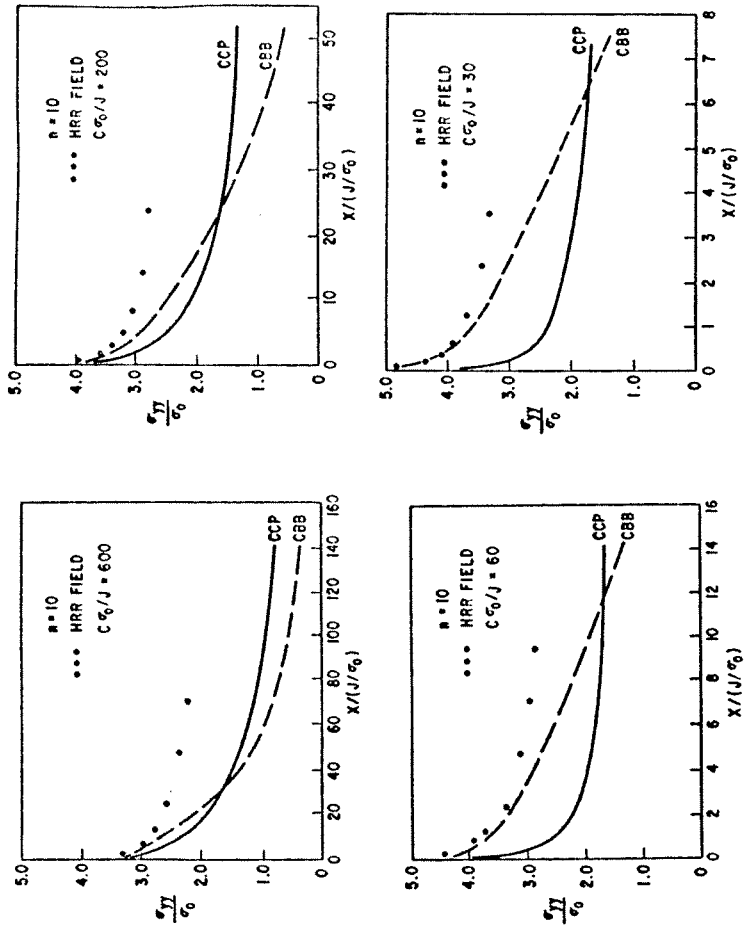
Fig. (14.6). Normal stress ahead of crack in CBB and CCP from contained to fully plastic conditions with $n = 10$, $\sigma_0/E = 0.002$ and $a/b = 0.75$.

15. RELATIONSHIP BETWEEN δ_t AND J UNDER J-DOMINATED CONDITIONS

References: D.M. Tracey, J. Eng. Mat. and Technology, 98, 1976, 146.

C.F. Shih, "Relationships between Crack Initiation and Growth Parameters Based on the J-Integral and the Crack Opening Displacement", Oct. 1978, G.E. Tech. Information Series, to be published.

The separation between the opened crack faces according to the J-fields (10.6) and (10.10) will be denoted by $\delta(r)$. The relative displacement of the faces to the tip in the x-direction is u_x . These are given by
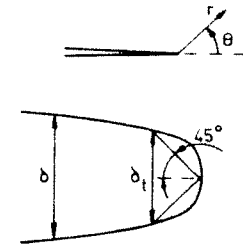
Fig. (15.1).

$$(u_x , \delta) = \alpha\varepsilon_0 \left[\frac{J}{\alpha\sigma_0\varepsilon_0 I_n}\right]^{\frac{n}{n+1}} r^{\frac{1}{n+1}} [\tilde{u}_x(\pi , n) , 2\tilde{u}_y(\pi , n)] \qquad (15.1)$$

Only in the limit $n \to \infty$ is there a nonzero value of δ as $r \to 0$. Rice (see Tracey, 1976) has suggested a definition for δ_t to be used for both hardening and nonhardening materials. As depicted in Fig. (15.1) δ_t is taken as the opening at the intercepts of the two $45°$ lines drawn back from the tip of the deformed profile, that is where

$$r - u_x = \delta/2 \qquad (15.2)$$

Solving (15.2) and (15.1) for this value of δ gives

$$\delta_t = d(\varepsilon_0, n) J/\sigma_0 \qquad (15.3)$$

where

$$d(\varepsilon_0, n) = (\alpha\varepsilon_0)^{\frac{1}{n}} (\tilde{u}_x + \tilde{u}_y)^{\frac{1}{n}} 2\tilde{u}/I_n \qquad (15.4)$$

Shih (1978) has computed d for both plane stress and plane strain. Plots are shown in Figs. (15.2) and (15.3) where ε_0 is identified with σ_0/E. Note that $\alpha = 1$ in these plots. In both cases the influence of strain hardening is
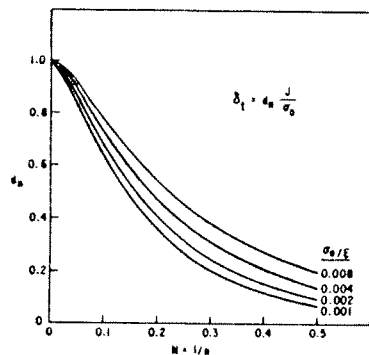
Fig. (15.2). Variation of d_n with n and σ_0/E for plane stress with $\alpha = 1$.
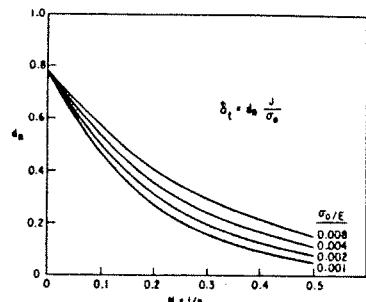
Fig. (15.3). Variation of d_n with n and σ_0/E for plane strain with $\alpha = 1$.

large. In plane stress the limit of the HRR singularity as $n \to \infty$ appears to be $\delta_t = J/\sigma_0$ which is the same as the Dugdale result (9.5), although there is no obvious reason why these should be the same. In plane strain the limit as $n \to \infty$ according to Shih's HRR singularity results from Fig. (15.3) is $\delta_t = .78 J/\sigma_0$. There is considerable variation in the published finite element results for the relation between δ_t and J (or K) in s.s.y. for the elastic-perfectly plastic case. Rice and Sorensen (J. Mech. Phys. Solids, 26, 1978, pg. 163) give a comparison of results, not including Shih's results presented here. Table (15.1) taken from Shih's

σ_0/E	n = 3	n = 5	n = 10	n = ∞
From Eq. 5 (HRR Singularity) .001	.13	.27	.46	.78
.002	.17	.31	.50	.78
.004	.21	.36	.53	.78
Flow Theory .002	.18	.29	.48	.63-.66
Deformation Theory .002	.20	.32	.52	.70
Tracey-Parks [31] .001	-	.30	.47	.65
Sorensen [31] .001	-	.27	.47	.66
McMeeking [31] .003	-	.27-.30	.41-.44	.55-.67
Cracked Bend Bar Fully Plastic .002	.19	-	.49	.58-.65
Center Cracked Panel Fully Plastic .002	.22	-	.64	.82-.87

Table 15.1.

Comparison of Values of $\delta_t/(J/\sigma_0)$ for Range of σ_0/E and n for Plane Strain*.

paper compares results for plane strain from various sources – reference [31] in the Table is the Rice-Sorensen paper. As expected, the finite element results for the fully plastic center-cracked panel are not in line with the other results because J-dominance was not acheived. For the other cases there is reasonable consistency among the results, except for the elastic-perfectly plastic limit where d ranges between about .55 and .8 .

Further comparisons of the results from (15.3) and l.s.y. finite element analyses can be found in the paper by Shih. Some comparisons between the theoretical predictions and measured $\delta_t - J$ relations are also given in this paper and reasonably good agreement is found. (The materials considered have hardening exponents ranging from $n = 5$ to $n = 13$).

* Unless otherwise indicated, $\delta_t/(J/\sigma_0)$ is determined from finite element calculations for small scale plasticity. In Ref. [31], calculations employ J_2 flow theory. The fully plastic analyses for the cracked bend bar, center cracked panel also employ J_2 flow theory.

16. CRACK GROWTH AND STABILITY UNDER J-CONTROLLED CONDITIONS

References: Paris, Tada, Zahoor and Ernst, "A Treatment of the Subject of Tearing Instability", U.S. N.R.C. Report NUREG-0311, August 1977.
Hutchinson and Paris, "Stability Analysis of J-Controlled Crack Growth", to be published in an ASTM-STP, 1978.

In general, the J-integral cannot be used to analyse crack growth in the l.s.y. range. (In the s.s.y. range J could equally well have been used instead of K in the analysis of Section 6). Crack growth involves elastic unloading and non-proportional plastic loading which is not properly modelled by a deformation theory of plasticity on which J is based. However, under restricted circumstances discussed below, small amounts of crack growth and its stability can be analysed. The approach is based on experimental data from a J-resistance curve and it closely parallels, and includes as a special case, the s.s.y. analysis of Section 6.

Conditions for J-controlled Growth

We consider materials with a J-resistance curve, $J_R(\Delta a)$, such as that in Fig. (16.1) which involves increasing J with increasing a. For many intermediate strength metals increases of J_R several times the initiation value J_c occurs after only a millimeter or two of crack growth - see, for example, Fig. (13.3). As depicted in Fig. (16.1), let D be the amount of growth necessary to double J above J_c calculated
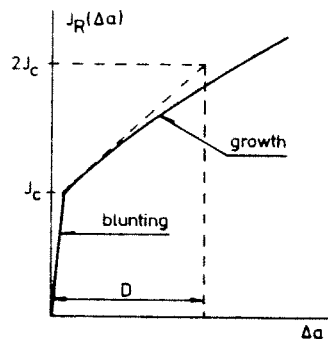
Fig. (16.1).

using the initial slope following initiation

$$D = J_c/(d J_R/da)_c \qquad (16.1)$$

Note that in s.s.y. D is exactly ½ the ℓ-quantity introduced on pg. 25.

We now consider the conditions under which the region of elastic unloading and non-proportional plastic flow will continue to be imbedded in J-dominated fields. The conditions sought are those which will guarantee the situation depicted in Fig. (16.2). With R denoting the size of the region in which the J-fields of deformation theory have dominance, one condition is obviously that

Fig. (16.2).

$$\Delta a << R \qquad (16.2)$$

The second condition follows from the requirement that nearly-proportional plastic loading occur within R but not, of course, right up to the tip. Consider the strain field (10.10) from the deformation theory solution, i.e.

$$\varepsilon_{ij} = k_n \, J^{\frac{n}{n+1}} \, r^{-\frac{n}{n+1}} \, \tilde{\varepsilon}_{ij} \qquad (16.3)$$

where k_n is a dimensional constant. The increments in the strains calculated from (16.3) for simultaneous increments in J and a are
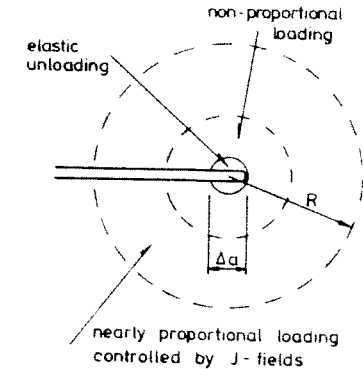
$$d\varepsilon_{ij} = k_n \, J^{\frac{n}{n+1}} \, r^{-\frac{n}{n+1}} \left[\frac{n}{n+1} \frac{dJ}{J} \tilde{\varepsilon}_{ij} + \frac{da}{r} \tilde{\beta}_{ij} \right] \qquad (16.4)$$

where

$$\tilde{\beta}_{ij} = \frac{n}{n+1} \cos\theta \, \tilde{\varepsilon}_{ij} + \sin\theta \frac{\partial}{\partial\theta} \tilde{\varepsilon}_{ij}$$

and where the change due to a is calculated as $-da(\partial(\ )/\partial x)$ since the crack tip is shifting ahead in the x-direction. The first term in the bracket in (16.4) corresponds to exactly proportional loading while the second, arising from da , is distinctly nonproportional. Since $\tilde{\varepsilon}_{ij}$ and $\tilde{\beta}_{ij}$ are of comparable magnitude, nearly proportional loading will occur where

$$da/r \ll dJ/J$$

Using the material-based length quantity D from (16.1) for growth just following initiation, this condition can be re-written as

$$D \ll r \qquad (16.5)$$

The second condition is therefore

$$D \ll R \qquad (16.6)$$

since this insures that there exists an annular region, as depicted in Fig. (16.2), $D \ll r \ll R$, in which nearly proportional loading holds and in which the J-fields control, or dominate, the actual behavior.

For a fully yielded configuration R will be some fraction of the uncracked ligament (or other relevant characteristic length) c . (As discussed in Section 14, R may be very small for certain configurations, eg. the centered-cracked strip in plane strain). The (16.6) can be written as

$$D \ll c \qquad (16.7)$$

or

$$\omega \equiv \frac{c}{D} = \frac{c}{J_R} \frac{d J_R}{d a} \gg 1 \qquad (16.8)$$

Only limited quantitative results are presently available for a more precise specification of the two conditions (16.2) and (16.8). Calculations by Shih, *et al.* (1978), shown in Figures (13.1) - (13.5), were carried out for the compact tension specimen of A533B steel. The calculations were carried out using J_2 flow theory. Nevertheless, J was found to be essentially path independent for the crack advancing as much as 5mm or 6% of the uncracked ligament, corresponding to increases in J above J_{Ic} of more than a factor of 5 . In addition, the calculated values of J agreed well with the experimentally measured values of J using the deformation theory formula (13.1). For their material and specimen $\omega \simeq 40$. Further work by Shih and Dean (to be published) indicates that values of ω as small as 10 may insure J-controlled growth in bend-type configurations, although this is a tentative result. Values for D in Table (16.1) introduced later range from a small fraction of a millimeter to centimeters, but for many of the intermediate strength metals D is on the order of a millimeter or less and thus (16.8) may often be met.

Stability of J-controlled Growth

Consider the general specimen under compliant loading in Fig. (8.1) where Δ_T is taken to be prescribed. Given the resistance curve of Fig. (16.1) the condition for continued crack growth, with Δa having already occured, is

$$J = J_R(\Delta a) \qquad (16.9)$$

With (16.9) satisfied the condition for stability of crack growth is

$$\left(\frac{\partial J}{\partial a}\right)_{\Delta_T} < \frac{dJ_R}{da} \qquad (16.10)$$

Paris, *et al.* (1977) introduced nondimensional quantities

$$T = \frac{E}{\sigma_0^2}\left(\frac{\partial J}{\partial a}\right)_{\Delta_T} \quad \text{and} \quad T_R = \frac{E}{\sigma_0^2}\frac{dJ_R}{da} \qquad (16.11)$$

and called T_R the _tearing modulus_ of the material. Stability is then insured if

$$T < T_R \qquad (16.12)$$

and instability sets in when equality is acheived. Values of T_R (T in the Table) and D are given in Table (16.1) for a number of materials based on values of dJ_R/da just following initiations. This Table is taken from Appendix II of Paris, *et al.* 1977. Note that T_R ranges from .1 to over 200 . (These values should only be regarded as preliminary estimates).

For later purposes, we now derive a general expression relating $(\partial J/\partial a)_{\Delta_T}$ to $(\partial J/a)_P$. Referring to Fig. (8.1), let $\Delta_T = \Delta + C_M P$. Regard Δ and J as functions of a and P . Thus, with Δ_T fixed,

$$\Delta_T = \left(\frac{\partial \Delta}{\partial a}\right)_P da + \left(\frac{\partial \Delta}{\partial P}\right)_a dP + C_M dP = 0$$

Then from

$$dJ = \left(\frac{\partial J}{\partial a}\right)_P da + \left(\frac{\partial J}{\partial P}\right)_a dP$$

and eliminating dP we obtain

$$\left(\frac{\partial J}{\partial a}\right)_{\Delta_T} = \left(\frac{\partial J}{\partial a}\right)_P - \left(\frac{\partial J}{\partial P}\right)_a\left(\frac{\partial \Delta}{\partial a}\right)_P\left[C_M + \left(\frac{\partial \Delta}{\partial P}\right)_a\right]^{-1} \qquad (16.13)$$

This generalizes (6.8) .

APPENDIX II
TABLE OF SOME MATERIAL PROPERTIES
(including "tearing modulus" - T)

MATERIAL	REF.	SPECIMEN TYPE	TEMP.	$\sigma_0 = \frac{\sigma_y + \sigma_{ult}}{2}$	J_{Ic}	$\frac{dJ}{da}$	$T = \frac{dJ}{da}\cdot\frac{E}{\sigma_0^2}$	D
			(F°)	(ksi)	($\frac{in\text{-}lbs}{in^2}$)	($\frac{lbs}{in^2}$)	(-)	(in)
ASTM-A469 (G.E.) rotor steel (Ni-Mo-V)	[7]	1"-c.t.	75°	95.9	(760)	-	-	
			100°	95.3	1260	$3.8 \times 10^-$	123.0	.03
			125°	94.5	-	3.0×10^4	101.0	
			150°	93.7	1340	3.8×10^4	130.0	.03
			175°	93.0	1050	3.6×10^4	124.0	
			250°	(88.0est.)	-	3.4×10^4	131.0	.03
			300°	80.0	720	2.8×10^4	131.0	.025
ASTM-A470 rotor steel (Cr-Mo-V)	[1]	1"-c.t.	300°	90.0	470	6.9×10^3	25.5	.07
			500°	90.0	413	7.0×10^3	25.8	.06
			800°	85.9	493	1.2×10^4	48.6	.04
ASTM-A471 rotor steel (Ni-Cr-Mo-V)	[2]	1"-c.t.	50°	146.1	860	1.45×10^4	20.4	.06
			150°	134.0	594	3.25×10^3	5.4	.16
			250°	128.5	670	6.54×10^3	11.9	
			250°	138.0	575	2.03×10^4	31.9	
			300°	125.0	500	1.47×10^4	27.9	
			500°	115.0	325	9.58×10^3	21.6	
			800°	104.0	325	8.75×10^3	24.1	.04
AISI-403 (12Cr-stainless) rotor steel	[3]	1"-c.t.	75°	109.0	572	7.1×10^3	17.9	
			200°	103.0	425	7.9×10^3	22.3	
			300°	96.3	460	7.3×10^3	23.6	
			500°	94.5	417	5.83×10^3	19.6	
			800°	86.2	372	4.08×10^3	16.5	
ASTM-A217 ($2\frac{1}{4}$ Cr-1Mo) cast steel	[4]	1"-c.t.	-50°	79.5	905	2.5×10^4	119.0	
			75°	71.9	860	1.89×10^4	109.0	
			300°	67.0	666	3.33×10^4	221.0	
			500°	64.5	433	2.40×10^4	172.0	
			800°	62.8	333	2.33×10^4	176.0	
ASTM-A453 (A286) (Discaloy) stainless steel	[2]	1"-c.t.	-452°	167.0	815	3.97×10^4	41.5	.02
			75°	135.0	692	2.0×10^4	32.8	
			400°	119.0	600	1.2×10^4	25.6	.05
			800°	112.0	517	9.3×10^3	22.4	
ASTM-A453 stainless steel (gas tongston arc welds)	[4]	1"-c.t.	-452°	107.8	1666.7	3.54×10^4	91.4	.05
ASTM-A540 (AISI 4340) steel	[2]	c.t.	-100°	(153.5est.)	600	3.7×10^4	47.1	.02
			50°	146.4	800	2.15×10^4	30.1	
			75°	145.5	652	2.10×10^4	29.8	
			250°	143.0	730	1.75×10^4	25.7	.07
			300°	142.5	720	1.0×10^4	14.8	
			550°	133.0	725	1.45×10^4	24.6	
Inco L.E.A. (low expansion alloy) sol'n treated and aged	[4]	c.t.	-452°	187.2	194	2.53×10^3	2.16	.08
			75°	137.2	263	1.07×10^3	1.71	

MATERIAL	CONDITION* REF.	SPECIMEN TYPE	TEMP.	$\sigma_0 = \frac{\sigma_y + \sigma_{ult}}{2}$	J_{IC}	$\frac{dJ}{da}$	$T = \frac{dJ}{da} \cdot \frac{E}{\sigma_0^2}$	D
6061-T651 Aluminum	[3]	1"-c.t.	75°	43.25	98.4	4.92×10^4	2.79	.2
310S stainless steel (shielded metal arc welds)	[4]	c.t.	-452°	152.9	336.5	1.03×10^4	13.27	.03
Inconel X750	[5] VIM-VAR/ST	c.t.	75°	120.4	320	4.64×10^3	10.2	.07
	DO-/ST	c.t.	-452°	127.0	240	1.72×10^3	3.6	
	DO-/STDA	c.t.	-452°	139.0	138	5.26×10^3	0.9	
	AAM-VAR/STDA		-452°	184.0	135	5.09×10^3	50.4	
	VIM-/STDA		-452°	213.7	500	2.06×10^4	15.1	
	HIP---		-452°	172.6	465	4.57×10^4	51.4	
	HIP-/STDA		-452°	185.3	233	1.89×10^4	18.4	
AISI-310S stainless steel	[6] STQ sensitized		-452°	154.0	1600	1.2×10^2	0.15	13.3
			-452°	152.0	675	7.5×10^4	97.1	
Kromarc-58 stainless steel	[6] Cw(L-t)	c.t.	-452°	227.3	452	3.0×10^3	1.74	.15
	Cw(T-L)		-452°	216.0	388	1.0×10^4	6.43	
	STQ(T-L)		-452°	175.0	1250	2.0×10^3	1.96	.62
	[4] GTAW	c.t.	-452°	181.4	615.5	9.3×10^3	8.48	
	Cw/GTAW	½ thick		199.9	725	9.17×10^3	6.89	
	GTAW/CN			214.2	216.7	2.71×10^4	1.77	
	GTAW/Cw/AN*			199.0	429	1.95×10^4	14.8	
	GTAW/Cw/AN**			175.7	812	3.62×10^4	35.19	
Inconel 706	[4] VIM-EFR/STDA	c.t.	-452°	211.5	530	1.21×10^4	8.13	.04
	VIM-VAR/STDA		-452°	207.0	660	1.94×10^4	13.6	
			75°	166.0	357	1.88×10^4	20.45	
Pyromet 538 (21Cr-6Ni-9Mn) stainless steel	[4] GATW		-452°	209.1	166	5.19×10^2	0.35	.32
			-452°	137.3	862.3	3.27×10^4	51.69	

*Denotes following material conditions
VIM-VAR-Vacuum induction melted followed by vacuum arc remelt.
AAM-VAR-Air arc melted followed by vacuum arc remelt.
VIM - Vacuum induction melted.
GTAW - Gas tungsten arc welds.
SMAW - Shielded metal arc welds.

** Denotes following heat treatments
ST - Solution treat.
STDA - Solution treat and double aged.
CW - Cold worked, 30% reduction in thickness.
STQ - 2000°F-1 hour- water quench

Next we will present some specific results for the deeply-cracked strip in three-point bending shown in Fig. (16.3). An analysis, essentially identical to that in Section 12, gives

Fig. (16.3).

$$J = \frac{2}{c} \int_0^{\Delta_{cr}} P \, d\Delta_{cr} \quad (16.14)$$

where $\Delta = \Delta_{nc} + \Delta_{cr}$. This result is not strictly correct under increasing crack length. As shown in Hutchinson and Paris (1978) the correct expression for J under increasing a is

$$J = 2 \int_0^{\Delta_{cr}} \frac{P}{c} \, d\Delta_{cr} - \int_{a_0}^{a} \frac{J}{c} \, da \qquad (16.15)$$

where a_0 is the initial crack length. For small amounts of growth with $\omega \gg 1$, the difference between (16.15) and (16.14) will usually be small.

Carrying out an analysis similar to that in Section 12 by making use of a nondimensional function similar to (12.2) for deeply-cracked strips, one can show

$$\left(\frac{\partial J}{\partial a}\right)_P = \frac{4P^2}{c^2}\left(\frac{\partial \Delta_c}{\partial P}\right)_a - \frac{J}{c}$$

Using the above expression in (16.13) and after some rearrangement, one can show that (see Hutchinson and Paris)

$$\left(\frac{\partial J}{\partial a}\right)_{\Delta_T} = \frac{4P^2}{c^2}\left[\frac{C}{1 + C\left(\frac{\partial P}{\partial \Delta_{cr}}\right)_a}\right] - \frac{J}{c} \qquad (16.16)$$

where $C = C_M + C_{nc}$ is the combined compliance. Up to and including initiation, all quantities on the right hand side of (16.16) can be measured directly from a load-displacement record; C is assumed known. The quantity $(\partial P/\partial \Delta_{cr})_a$ is
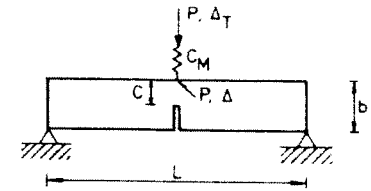
continuous at initiation but cannot be measured directly once grow takes place. In (16.10), $(\partial J/\partial a)_{\Delta_T}$ from (16.16) provides a check on stability at initiation which can be assessed directly from the experimental record.

For a fully yielded strip of a nonhardening material P is the limit load and $(\partial P/\partial\Delta_{cr})_a = 0$. Then (16.16) reduces to

$$\left(\frac{\partial J}{\partial a}\right)_{\Delta_T} = \frac{4P^2C}{c^2} - \frac{J}{c} \tag{16.17}$$

The strong role of the combined compliance of the system on stability is obvious from this formula. The limit load for the strip of Fig. (16.3) is $P = 4A\sigma_0 c^2/L$ where $A = .364$ in plane strain and $A = .268$ in plane stress. Regarding the uncracked strip as a beam gives $C_{nc} = L^3/(4Eb^3)$. Then, from its definition in (16.11),

$$T = 16A^2 \frac{c^2 L}{b^3}\left(1 + \frac{C_M}{C_{nc}}\right) - \frac{EJ}{\sigma_0^2 c} \tag{16.18}$$

Paris, et al. (1977) have tested a number of specimens under three-point bending in series with a beam of variable compliance as depicted in Fig. (16.4). The compliance of the test machine is negligible compared to the combined compliance of the specimen and the beam so the relative displacement of the machine heads Δ_T is prescribed. Using (16.16) and data directly from the experimental load-deflection record, the value of T ($T_{applied}$) at initiation ranged from about zero when the beam was absent to a value of just under 50 for the longest beam. (Note that the notation for b and L in Fig. (16.4) is different from that in Fig. (16.3)). The value of T_R (T_{mat}) just following initiation was 36 and the ω parameter in (16.8) is about 15. For each specimen the point (T, T_R) is plotted in the Figure and it is shown as a solid point if fracture initiation was observed to be stable and as and open point if unstable. The solid line $T = T_R$ is the theoretical dividing line for stability and instability from (16.12).
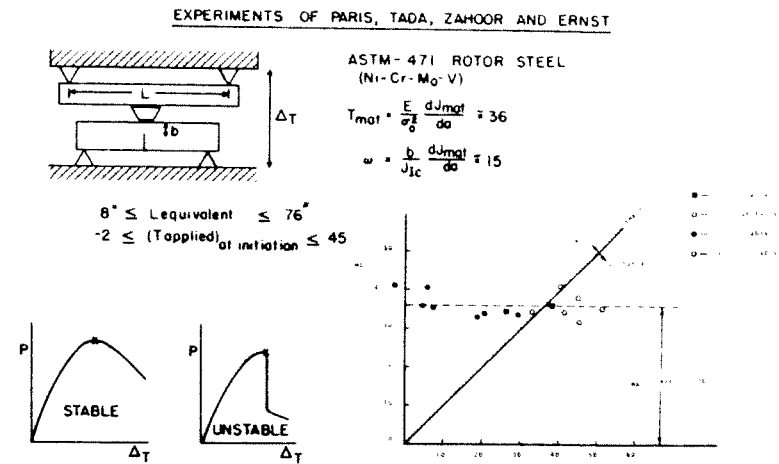
EXPERIMENTS OF PARIS, TADA, ZAHOOR AND ERNST

ASTM-471 ROTOR STEEL (Ni-Cr-Mo-V)

$T_{mat} = \frac{E}{\sigma_f^2}\frac{dJ_{mat}}{da} = 36$

$\omega = \frac{b}{J_{Ic}}\frac{dJ_{mat}}{da} = 15$

$8° \leq L_{equivalent} \leq 76°$

$-2 \leq (T_{applied})_{at\ initiation} \leq 45$

Fig. (16.4).

The significance of the large T_R values for intermediate strength metals ($T_R \geq 30$, say) is that in many situations the T-value will be considerably smaller than T_R so that small amounts of crack growth can be tolerated. For example, the s.s.y. result for the finite crack of length $2a$ in an infinite body under tensile stress σ^∞ has $J = \pi a(\sigma^\infty)^2/E$ and

$$T = \pi(\sigma^\infty/\sigma_0)^2$$

Thus, T for this problem in s.s.y. will never exceed about 1. Next consider a finite crack of length $2a$ in an infinite body under fully plastic conditions. From fully plastic solutions such as those in Section 12, where in plane strain tension $\epsilon/\epsilon_y = (\sigma/\sigma_y)^n$,

$$J = \sigma_y \epsilon_y\, a\, h(n)\, (\sigma^\infty/\sigma_y)^{n+1} = \sigma_y \epsilon_y\, a\, h(n)\, (\epsilon^\infty/\epsilon_y)^{\frac{n+1}{n}}$$

where $h \approx 3$ for $n = 10$ - see Hutchinson, et al. (pg. 59).

Under these conditions

$$T = h(n) (\varepsilon^{\infty}/\varepsilon_y)^{\frac{n+1}{n}}$$

and T will only reach values as large as 30, say, for $\varepsilon^{\infty} \gtrsim 10\varepsilon_y$. Of course, when a crack extends across a significant fraction of a cross-section and the loading conditions approach dead loading, then T will be large as illustrated by the analysis of the 3-point bend bar.

17. SOURCE OF STABLE CRACK GROWTH

References: F.A. McClintock and G.R. Irwin, ASTM STP 381, 1965, pg. 84.

A.D. Chitaley and F.A. McClintock, JMPS, 19, 1971, pg. 147.

J.R. Rice, in Fracture, Volume II, 1968, pg. 277.

J.R. Rice and E.P. Sorensen, JMPS, 26, 1978, pg. 163.

In this section the problem of a crack growing quasi-statically in an elastic-perfectly plastic medium is considered. We start by contrasting the steady-state problem in Mode III with the stationary problem, both in s.s.y. Then the transient problem is treated with emphasis on the tearing resistance of the material immediately following initiation. Lastly some recent work on the s.s.y., plane strain problem will be discussed.
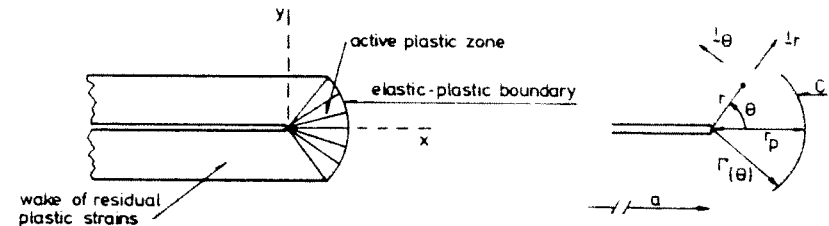
Steady-state crack growth in s.s.y. Mode III

Fig. (17.1).

We consider the steady-state situation depicted in Fig. (17.1) where the crack has grown under s.s.y. conditions such that to an observer traveling with the crack tip the stress and strain fields no longer change. Far from the tip (except

in the wake) the stresses are given by the elastic singularity
fields, i.e.,

$$(\tau_r , \tau_\theta) = K(2\pi r)^{-1/2}\left[\sin\tfrac{1}{2}\theta , \cos\tfrac{1}{2}\theta\right]$$

The material is assumed to be elastic-perfectly plastic with
the yield condition

$$\tau \equiv \sqrt{\tau_r^2 + \tau_\theta^2} = \tau_0 .$$

The analysis given below is due to McClintock and Irwin (1965).
The present version is largely taken from the fracture article
by Rice (1968), using results from the more recent paper by
Chitaley and McClintock (1971), but contact will be made with
the results of the last few sections.

Let (˙) denote the material derivative with respect to
the increase in crack length, i.e. $\partial( )/\partial a$. If $f(x , y)$
denotes the instantaneous spatial variation of any quantity in
steady-state, then

$$\dot{f} = - \partial f/\partial x \qquad (17.1)$$

In the active plastic zone ahead of the tip equilibrium and
yielding, plus a focussing of the strain-rate, requires the
same fan of slip lines as in the stationary problem (see Fig.
(11.1)) with

$$\underset{\sim}{\tau} \equiv \tau_r \underset{\sim}{i}_r + \tau_\theta \underset{\sim}{i}_\theta = \tau_0 \underset{\sim}{i}_\theta \qquad (17.2)$$

With $\dot{\underset{\sim}{\gamma}} = \dot{\gamma}_x \underset{\sim}{i}_x + \dot{\gamma}_y \underset{\sim}{i}_y = \dot{\gamma}_r \underset{\sim}{i}_r + \dot{\gamma}_\theta \underset{\sim}{i}_\theta$ as the strain-
rate vector which in steady-state is given by

$$\dot{\underset{\sim}{\gamma}} = \underset{\sim}{\nabla}\dot{w} = - \underset{\sim}{\nabla}(\partial w/\partial x) = - \frac{\partial}{\partial r}\left(\frac{\partial w}{\partial x}\right)\underset{\sim}{i}_r - \frac{1}{r}\frac{\partial}{\partial\theta}\left(\frac{\partial w}{\partial x}\right)\underset{\sim}{i}_\theta \qquad (17.3)$$

the constitutive law is

$$\dot{\underset{\sim}{\gamma}} = \dot{\underset{\sim}{\gamma}}^e + \dot{\underset{\sim}{\gamma}}^P = \dot{\underset{\sim}{\tau}}/G + \lambda(r , \theta)\underset{\sim}{\tau} = \dot{\underset{\sim}{\tau}}/G + \lambda \tau_0 \underset{\sim}{i}_\theta \qquad (17.4)$$

Now,

$$\dot{\underset{\sim}{\tau}} = \tau_0 \dot{\underset{\sim}{i}}_\theta = - \tau_0 \partial(\underset{\sim}{i}_\theta)/\partial x = - \tau_0 r^{-1}\sin\theta \underset{\sim}{i}_r \qquad (17.5)$$

Using (17.3) and (17.5) in (17.4) and equating components, we
find (with $\gamma_0 = \tau_0/G$)

$$\frac{\partial}{\partial r}\left(\frac{\partial w}{\partial x}\right) = \gamma_0 \frac{\sin\theta}{r} , \quad \frac{1}{r}\frac{\partial}{\partial\theta}\left(\frac{\partial w}{\partial x}\right) = - \lambda \tau_0 \qquad (17.6)$$

The general solution to the first of (17.6) is

$$\gamma_x = \partial w/\partial x = \gamma_0 \sin\theta \ln r + F(\theta) \qquad (17.7)$$

To determine $F(\theta)$ note that on the elastic-plastic boundary
$\underset{\sim}{\gamma} = \underset{\sim}{\tau}/G$ (since $\underset{\sim}{\gamma}^P = 0$) , i.e. for $r = \Gamma(\theta)$

$$\underset{\sim}{\gamma} = \gamma_0 \underset{\sim}{i}_\theta = \gamma_0\left[- \sin\theta \underset{\sim}{i}_x + \cos\theta \underset{\sim}{i}_y\right]$$

Thus on C $\gamma_x = - \gamma_0 \sin\theta$ so that

$$F = - \gamma_0 \sin\theta(1 + \ln \Gamma(\theta))$$

and therefore in the active zone

$$\gamma_x = - \gamma_0 \sin\theta\left[1 + \ln(\Gamma(\theta)/r)\right] \qquad (17.8)$$

Since $\partial \gamma_y/\partial x = \partial \gamma_x/\partial y$, from (17.8) we obtain <u>for $\theta = 0$
ahead of the crack tip</u> $(\partial( )/\partial x = \partial( )/\partial r$ and $\partial( )/\partial y = r^{-1}\partial( )/\partial\theta)$

$$\frac{\partial \gamma_\theta}{\partial r} = \frac{1}{r}\frac{\partial \gamma_x}{\partial\theta} = - \frac{\gamma_0}{r}\left[1 + \ln\left(\frac{r_p}{r}\right)\right] \qquad (17.9)$$

where $r_p = \Gamma(\theta = 0)$. Finally integrate (17.9) subject to
$\gamma_\theta = \gamma_0$ at $r = r_p$ with the resulting strain distribution
directly ahead of the crack in the active plastic zone

$$\gamma_\theta = \gamma_0\left[1 + \ln(r_p/r) + \tfrac{1}{2}\ln^2(r_p/r)\right] \qquad (17.10)$$

This result can be contrasted with the corresponding strain distribution directly ahead of the crack in the stationary problem from (11.14)

$$\gamma_\theta = \gamma_0(\bar{r}_p/r) \qquad (17.11)$$

where $\bar{r}_p$ is the distance to the elastic-plastic boundary in the stationary problem. Chitaley and McClintock (1971) have carried out a detailed numerical analysis of the s.s.y., steady-state problem in Mode III. They find that to within about 5%

$$r_p = \bar{r}_p = \frac{1}{\pi}\left(\frac{K}{\tau_0}\right)^2 = \frac{2}{\pi}\frac{J}{\tau_0\gamma_0} \qquad (17.12)$$

and in the subsequent discussion we will take (17.12) to hold.

The singularity in the stationary problem is much stronger than for the growing crack. At the <u>same value of K</u> (or J) the strain near the tip (i.e., $r/r_p \ll 1$) is considerably larger in the stationary problem. In Fig. (17.2) a plot is given of

$$\frac{(\gamma_\theta)_{s.s.}}{(\gamma_\theta)_{stat.}} = \frac{r}{r_p}\left[1 + \ln(r_p/r) + \tfrac{1}{2}\ln^2(r_p/r)\right] \qquad (17.13)$$

The lower strain levels in the growing crack problem result from the distinctly nonproportional plastic deformation which occurs in the active plastic zone. An elastic-plastic material has considerable resistance to nonproportional straining as compared to a nonlinear elastic solid. This is the source of the stable crack growth. For example, note from (17.4) that the plastic part of the strain-rate is constrained to have only an $\dot{\imath}_\theta$ - component. For a true deformation theory of plasticity there is no difference between the strains in the stationary problem and the growing problem at the same value of J .
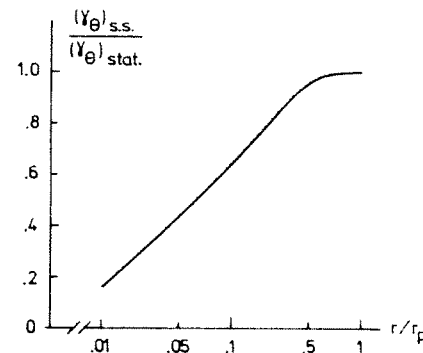
Fig. (17.2).

To further explore the implications of the steady-state solution vs. the stationary solution, McClintock and Irwin proposed the following "microscopic" critical strain condition for initiation and continued growth in Mode III

$$\gamma_\theta = \gamma_c \quad \text{at} \quad r = r_c \qquad (17.14)$$

in the plastic zone ahead of the crack. (Here we use total strain; McClintock and Irwin used plastic strain). For <u>initiation</u> this implies from (17.11) and (17.12)

$$J_c = \frac{\pi}{2}r_c\gamma_c\tau_0 \quad \text{and} \quad r_p^c = \alpha r_c \qquad (17.15)$$

where $\alpha = \gamma_c/\gamma_0$. For <u>steady-state growth</u> the criterion implies, using (17.10),

$$\gamma_c = \gamma_0\left[1 + \ln(r_p/r_c) + \tfrac{1}{2}\ln^2(r_p/r_c)\right]$$

Solving for r_p/r_c in the above and using (17.12), one finds

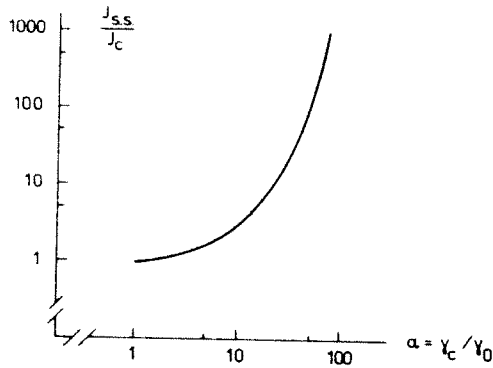$$J_{ss} = \frac{\pi}{2}r_c\gamma_0\tau_0 \exp[\sqrt{2\alpha-1} - 1] \qquad (17.16)$$

Fig. (17.3).

Thus,

$$\frac{J_{ss}}{J_c} = \frac{1}{\alpha} \exp[\sqrt{2\alpha - 1} - 1]$$ (17.17)

A plot of this ratio is shown in Fig. (17.3). For $\alpha = 10$, $J_{ss} \stackrel{\sim}{=} 3J_c$. For even larger values of α, J_{ss} becomes very much larger than J_c. Note that for relatively "brittle" materials where $1 < \alpha < 10$, J_{ss} is not substantially above J_c and $J_{ss} = J_c$ for $\alpha = 1$.

Initiation and subsequent growth in s.s.y. Mode III

We now consider the transient problem starting from the crack prior to growth and analysing the subsequent growth. At an appropriate point the fracture criterion (17.14) will again be invoked. The distance to the elastic-plastic boundary $\Gamma(\theta, a)$ is now a function of a and θ. Again, let $(\dot{\ })$ denote the material derivative with respect to a. Eq. (17.4) still stands and $\dot{\underset{\sim}{\tau}}$ is still given by (17.5) since $\underset{\sim}{\tau} = \tau_0 \underset{\sim}{i}_\theta$ in the plastic zone. Since

$$\dot{\underset{\sim}{\gamma}} = \nabla \dot{w} = \frac{\partial \dot{w}}{\partial r} \underset{\sim}{i}_r + \frac{1}{r} \frac{\partial \dot{w}}{\partial \theta} \underset{\sim}{i}_\theta ,$$

Eq. (17.4) implies

$$\frac{\partial \dot{w}}{\partial r} = -\gamma_0 \sin\theta r^{-1} \quad \text{and} \quad \frac{\partial \dot{w}}{\partial \theta} = \lambda \tau_0 r$$ (17.18)

The first of these equations can be differentiated to give

$$\frac{\partial}{\partial r}(r \dot{\gamma}_\theta) = \frac{\partial^2}{\partial \theta \partial r} \dot{w} = -\gamma_0 \cos\theta r^{-1}$$

which then integrates to

$$\dot{\gamma}_\theta = -\gamma_0 \cos\theta r^{-1} \ell n \, r + r^{-1} F(\theta)$$

With $(\dot{\gamma}_\theta)_C$ denoting the value of $\dot{\gamma}_\theta$ at the current location of C, this can be rewritten as

$$\dot{\gamma}_\theta = \gamma_0 \cos\theta r^{-1} \ell n(\Gamma/r) + (\Gamma/r) (\dot{\gamma}_\theta)_C$$ (17.19)

Directly ahead of the crack $(\theta = 0, \Gamma = r_p)$ this specializes to

$$\dot{\gamma}_\theta = \gamma_0 r^{-1} \ell n(r_p/r) + (r_p/r) (\dot{\gamma}_\theta)_{r_p}$$ (17.20)

To calculate the last term note that $\gamma_\theta = \gamma_0$ on C, since $\underset{\sim}{\gamma} = \underset{\sim}{\tau}/G = \gamma_0 \underset{\sim}{i}_\theta$. Let $D\gamma_\theta/Dt$ denote the derivative of γ_θ following the elastic-plastic boundary. Since $(\dot{\gamma}_\theta)_{r_p}$ is the material derivative of γ_θ, ahead of the crack these two derivatives are related by

$$\frac{D\gamma_\theta}{Dt} = (\dot{\gamma}_\theta)_{r_p} + \left(\frac{\partial\gamma_\theta}{\partial r}\right)_{r_p} (1 + \dot{r}_p) = 0$$

where in the convective term $d(a + r_p)/da = 1 + \dot{r}_p$. Now,

$$\frac{\partial\gamma_\theta}{\partial r} = \frac{\partial}{\partial r}\left(\frac{1}{r}\frac{\partial w}{\partial \theta}\right) = -\frac{1}{r}\gamma_\theta + \frac{1}{r}\frac{\partial\gamma_r}{\partial \theta}$$

so that $(\partial\gamma_\theta/\partial r)_{r_p} = -\gamma_0/r_p$ (since $\gamma_\theta = \gamma_0$ and $\gamma_r = 0$ on

C) . Therefore,

$$(\dot{\gamma}_\theta)_{r_p} = \gamma_0 \, r_p^{-1} (1 + \dot{r}_p)$$

Using this in (17.20) gives

$$\dot{\gamma}_\theta = \gamma_0 r^{-1} [1 + \ln(r_p/r)] + \gamma_0 r^{-1} \dot{r}_p \qquad (17.21)$$

or

$$d\gamma_\theta = \gamma_0 r^{-1} [1 + \ln(r_p/r)] da + \gamma_0 r^{-1} dr_p \qquad (17.22)$$

The first term in (17.21) or (17.22) is exactly the same as the steady-state contribution - see (17.9) - with no change in r_p ; while the second term can be thought of as that due to a stationary crack with increasing r_p - see (17.11).

Again we invoke s.s.y. and assume (17.12) provides a good approximation to r_p - see for example H. Andersen, JMPS, 21, 1973, pg. 337 and E.P. Sorensen, Int. J. Fracture, 14, 1978, pg. 485. Since $dr_p = 2dJ/(\pi \gamma_0 \tau_0)$, (17.22) becomes

$$d\gamma_\theta = \gamma_0 r^{-1} [1 + \ln(r_p/r)] da + 2dJ/(\pi \tau_0 r)$$

We now adopt the near-tip fracture criterion (17.14). Consider <u>initiation and the first increment of growth</u>. Again with $\alpha = \gamma_c/\gamma_0$,

$$(r_p)_c = \frac{2}{\pi} \frac{J_c}{\gamma_0 \tau_0} = \alpha r_c \qquad (17.23)$$

and

$$\gamma_\theta = \gamma_c r_c r^{-1} \qquad (17.24)$$

Assume (17.23) and (17.24) pertain such that initiation is possible. Regard the strain ahead of the crack as a function of x , which is fixed to the material points and chosen to coincide with r before growth and a , i.e. $\gamma_\theta(x , a)$. The

condition which is currently met is $\gamma_\theta(r_c , a) = \gamma_c$; after an increment of growth da we require $\gamma_\theta(r_c + da , a + da) = \gamma_c$. This is

$$\gamma_\theta(r_c + da , a + da) = \gamma_\theta(r_c , a) + \dot{\gamma}_\theta(r_c , a) da + \frac{\partial \gamma_\theta}{\partial x}(r_c , a) da = \gamma_c$$

or

$$\dot{\gamma}_\theta(r_c , a) = - \frac{\partial \gamma_\theta}{\partial x}(r_c , a) = \frac{\gamma_c}{r_c}$$

where the last equality follows from (17.24).

Using (17.21) in the above with (17.23) we find

$$\dot{r}_p = \alpha - 1 - \ln \alpha \qquad (17.25)$$

or, from (17.12),

$$\left(\frac{dJ}{da}\right)_c = \frac{\pi}{2} \tau_0 \gamma_0 (\alpha - 1 - \ln \alpha) \qquad (17.26)$$

This provides the <u>tearing modulus</u> at initiation

$$T_R = \frac{G}{\tau_0^2} \left(\frac{dJ}{da}\right)_c = \frac{\pi}{2}(\alpha - 1 - \ln \alpha) \qquad (17.27)$$

A "perfectly brittle" material with $\alpha = 1$ corresponds to $T_R = 0$; while for large α , $T_R \approx \pi\alpha/2$. Similarly the material-based length quantity, D , introduced in (16.1) is given by

$$D = \frac{J_c}{(dJ/da)_c} = r_c \frac{\alpha}{\alpha - 1 - \ln \alpha}$$
$$\qquad (17.28)$$
$$\cong r_c \text{ for } \alpha > 10$$

Thus for a material with a large tearing modulus ($\alpha > 10$, $T_R > 15$) the distance D needed to double J above J_c is essentially r_c , which can be thought of as the size of the fracture process zone in the present context.

The model suggests certain implications relating macro-

scopic fracture resistance to features of the fracture process zone. In particular, note that the ratio, J_{ss}/J_c , in (17.17) and the nondimensional tearing modulus T_R in (17.27) depend only on $\alpha = \gamma_c/\gamma_0$. Furthermore, for large α J_{ss}/J_c increases exponentially while T_R increases linearly in α . Note that for $\alpha = 60$, $T_R \cong 100$ and $J_{ss}/J_c \cong 1000$. For larger values of α the small strain assumptions will certainly be violated for typical values of γ_0 at the point where $r = r_c$. But the model does suggest the source of the large values of T_R which are observed experimentally in plane strain. The very large values of J_{ss}/J_c for large α result from the considerable resistance an elastic-plastic material offers to nonproportional straining, as has already be noted. This effect is undoubtedly <u>overestimated</u> by the simple smooth yield surface of Mises (and Tresca in Mode III) used in the present analysis. In this sense the values of J_{ss}/J_c for large α may be considerably in excess of observable values.

Starting from (17.22) it is possible to set up the problem for calculating the entire resistance curve $J_R(\Delta a)$; we have only determined its initial slope and its asymptote. See McClintock and Irwin (1965) and Rice (1968) for an approximate determination of the whole curve.

Rice and Sorensen (1978) have considered the more difficult Mode I, plane strain problem in s.s.y. Qualitatively the findings are similar to Mode III and several features of the analysis are closely analogous. The authors assume that the near-tip stress field is still the Prandtl slip line field under growing conditions. This is not obvious in plane strain but they present numerical results which suggest the plausibility of the assumption. While the criterion (17.14) is sensible in Mode III, a critical condition cannot be taken to be met ahead of the crack in plane strain Mode I since the strains are most intense above and below the tip in the small strain solution. Instead, Rice and Sorensen used an alternative criterion which is essentially an integration of the near-tip strains. They require the crack opening displacement to reach a critical value at some fixed small distance back behind the tip. By making contact with numerical results they are able to

obtain an approximate integration of the equations relating the crack opening displacement, the crack advance and J . Resistance curves are determined. Large tearing resistance is found, typical of observed values, with realistic choices for the near-tip fracture criterion.